BBA - Molecular Basis of Disease 1868 (2022) 166398

Contents lists available at ScienceDirect

BBA - Molecular Basis of Disease

journal homepage: www.elsevier.com/locate/bbadis

# Kupffer cells are protective in alcoholic steatosis☆

Nikolai Köhler[a,1], Marcus Höring[b,1], Beate Czepukojc[c,1], Tim Daniel Rose[a,1], Christa Buechler[d], Tarek Kröhler[c], Johannes Haybaeck[e,f], Gerhard Liebisch[b], Josch K. Pauling[a,*], Sonja M. Kessler[c,g,**], Alexandra K. Kiemer[c,*]

[a] Bavarian Institute for Digital Transformation, Chair of Experimental Bioinformatics, TUM School of Life Sciences Weihenstephan, Technical University of Munich (TUM), 85354 Freising, Germany
[b] Institute for Clinical Chemistry and Laboratory Medicine, University of Regensburg, 93053 Regensburg, Germany
[c] Department of Pharmacy, Pharmaceutical Biology, Saarland University, 66123 Saarbrücken, Germany
[d] Internal Medicine I, University Hospital of Regensburg, 93053 Regensburg, Germany
[e] Institute of Pathology, Neuropathology, and Molecular Pathology, Medical University of Innsbruck, Innsbruck, Austria
[f] Diagnostic & Research Center for Molecular Biomedicine, Institute of Pathology, Medical University of Graz, Graz, Austria
[g] Institute of Pharmacy, Experimental Pharmacology for Natural Sciences, Martin Luther University Halle-Wittenberg, 06120 Halle, Germany

ARTICLE INFO

*Keywords:*
Lieber-DeCarli diet
Lipidomics
Macrophages
Phospholipids
Sphingolipids
Bi-clustering
Louvain communities

ABSTRACT

Massive accumulation of lipids is a characteristic of alcoholic liver disease. Excess of hepatic fat activates Kupffer cells (KCs), which affect disease progression. Yet, KCs contribute to the resolution and advancement of liver injury. Aim of the present study was to evaluate the effect of KC depletion on markers of liver injury and the hepatic lipidome in liver steatosis (Lieber-DeCarli diet, LDC, female mice, mixed C57BL/6J and DBA/2J background). LDC increased the number of dead hepatocytes without changing the mRNA levels of inflammatory cytokines in the liver. Animals fed LDC accumulated elevated levels of almost all lipid classes. KC ablation normalized phosphatidylcholine and phosphatidylinositol levels in LDC livers, but had no effect in the controls. A modest decline of trigylceride and diglyceride levels upon KC loss was observed in both groups. Serum aminotransferases and hepatic ceramide were elevated in all animals upon KC depletion, and in particular, cytotoxic very long-chain ceramides increased in the LDC livers. Meta-biclustering revealed that eight lipid species occurred in more than 40% of the biclusters, and four of them were very long-chain ceramides. KC loss was further associated with excess free cholesterol levels in LDC livers. Expression of inflammatory cytokines did, however, not increase in parallel. In summary, the current study described a function of KCs in hepatic ceramide and cholesterol metabolism in an animal model of LDC liver steatosis. High abundance of cytotoxic ceramides and free cholesterol predispose the liver to disease progression suggesting a protective role of KCs in alcoholic liver diseases.

*Abbreviations:* ALT, alanine aminotransferase; AST, aspartate aminotransferase; CE, cholesteryl ester; *Clec4f*, C-Type Lectin Domain Family 4 Member F; DG, diglycerides; *Elovl6*, fatty acid elongase 6; *Fasn*, fatty acid synthase; *Hmgcr*, 3-hydroxy-3-methylglutaryl coenzyme A *reductase*; Il, interleukin; KC, Kupffer cells; LDC, Lieber-DeCarli diet; LPC, lysophosphatidylcholine; LPE, lysophosphatidylethanolamine; MU, monounsaturated; PC, phosphatidylcholine; PE, phosphatidylethanolamine; PI, phosphatidylinositol; PS, phosphatidylserine; PU, polyunsaturated; TG, triglycerides; *Scd1*, stearoyl-CoA desaturase 1; UMAP, Uniform Manifold Approximation and Projection.

☆ Loss of Kupffer cells in alcoholic steatosis is associated with increased hepatic ceramide and free cholesterol levels

* Corresponding authors.
** Corresponding author at: Martin Luther University Halle-Wittenberg, Institute of Pharmacy, Experimental Pharmacology for Natural Sciences, 06120 Halle, Germany.
*E-mail addresses:* josch.pauling@wzw.tum.de (J.K. Pauling), sonja.kessler@pharmazie.uni-halle.de (S.M. Kessler), pharm.bio.kiemer@mx.uni-saarland.de (A.K. Kiemer).

[1] These authors contributed equally to this work.

https://doi.org/10.1016/j.bbadis.2022.166398
Received 6 October 2021; Received in revised form 15 March 2022; Accepted 16 March 2022
Available online 19 March 2022

## 1. Introduction

Ethanol abuse causes alcoholic liver disease ranging from fatty liver to hepatitis, liver fibrosis and cirrhosis [1,2]. Steatosis is the initial stage of alcoholic liver disease and is reversible with the abstinence from ethanol [1]. Disturbed hepatic lipid metabolism is a key feature of alcoholic liver disease, and liver steatosis is a risk factor for progressive liver damage [1].

Alcohol consumption is more prevalent in males, but the incidence is increasing in women [3,4]. Females respond differentially to toxins than men and are more susceptible to alcoholic liver injury [5]. Thus, liver steatosis and fibrosis have been reported to be higher in female than male mice exposed to ethanol for 4 weeks [6]. Most animal studies used male mice and adequate inclusion of female animals is essential to better understand disease pathology in both genders [7].

Metabolic dysfunction is a common cause of liver steatosis and a major risk factor for non-alcoholic fatty liver disease (NAFLD). Patients who have NAFLD and an excessive alcohol consumption have a higher risk to develop progressive liver disease. Prevalence of NAFLD is up to 30% in Western countries, and about 5% of adults in the United States have alcoholic fatty liver. Thus, 0.84% of the Americans have both, alcoholic and metabolic liver disease [8]. Alcoholic liver disease and NAFLD both range from steatosis to inflammation and to cirrhosis. Presence of metabolic syndrome increases the progression of alcoholic liver disease and alcohol intake promotes the advancement of NAFLD [9]. A significant overlap in disease pathogenesis exists, and in 2020 it was proposed to replace NAFLD by metabolic (dysfunction) associated fatty liver disease (MAFLD) [10]. In comparison to NAFLD, MAFLD does not require the exclusion of patients with excessive alcohol intake or viral hepatitis [8]. Notably, there are also considerable differences between alcoholic and non-alcoholic liver diseases, and these are related to functions associated with the immune response [9]. In alcoholics unsaturated rather than saturated dietary fats seem to be harmful suggesting that lipid metabolism may vary as well [11,12].

About 60 to 90% of patients with ethanol abuse have liver steatosis, and triglycerides accumulate in the liver [13,14]. Ethanol increases the hepatic uptake and synthesis of fatty acids and inhibits lipid oxidation, and this ultimately results in liver steatosis [1]. Ethanol consumption, moreover, induces adipose tissue dysfunction, thereby enhancing lipolysis in fat tissues and deposition of these fatty acids in peripheral organs, such as the liver [15]. Inflamed adipose tissues releases inflammatory cytokines and adipokines, which further advance liver injury [16–19].

Regarding that steatosis is a risk factor for progressive liver damage [1], detailed analysis of the hepatic lipidome may give important insights into the pathology of alcoholic liver disease.

Ceramides are bioactive sphingolipids that can induce apoptosis and modulate insulin signaling [20]. Hepatic ceramide levels were found increased in the human alcoholic liver [21]. In a rodent model using male Long Evans rats, higher hepatic concentrations of long-chain ceramides were described [22]. Upregulation of ceramide levels upon alcohol feeding was, however, not observed in a separate experimental study, which analyzed C57BL/6 mice [23].

Chronic ethanol consumption further increased hepatic cholesterol levels in deer mice. Notably, accumulation of esterified cholesterol and triglycerides was only observed in alcoholic dehydrogenase deficient animals [24]. In male C57BL/6 mice, where ethanol was applied by intragastric feeding, hepatic free cholesterol levels, and thus total cholesterol amount, even declined [25]. Notably, in male C57BL/6 mice and rats hepatic cholesterol levels were nevertheless found to increased upon chronic ethanol infusion [26].

Phosphatidylcholine (PC) regulates cholesterol trafficking pathways and feeding baboons ethanol combined with PC protected against liver fibrosis [27,28]. Rodent studies indeed described that hepatic PC levels declined in alcoholic liver disease [14,24]. The cholesterol/PC ratio in plasma membranes is essential for cell viability and cell signaling [27], and was disturbed in alcoholic liver disease [14,24,29].

It was also reported that C18:0 and C22:6 containing lipids increased in livers of mice fed the Lieber-DeCarli (LDC) diet, which represents a widely used model to investigate alcoholic liver disease [1,30]. Several studies identified a shift towards unsaturated acyl chains in rodent alcoholic liver, and levels of monounsaturated and polyunsaturated lipids were elevated [1]. Accumulation of unsaturated fat contributes to oxidative stress and progressive liver damage [20] and may promote liver injury.

Results regarding cholesterol and ceramide levels in murine alcoholic steatosis are disconcordant [25,26]. Age, gender, genetic, and environmental factors, which may all also affect the microbiome, are of key importance in the regulation of the hepatic lipid composition [14,31,32], and also have to be considered in experimental models for alcoholic liver diseases [33]. C57BL/6J and DBA/2J mice are commonly used mouse strains, greatly vary genetically and differently respond to alcohol [34–36]. Hybrid mice of these two strains are more resistant to diseases, live longer and have larger litters [37]. The better physical condition of these animals may be an advantage over the inbred progenitor strains when studying alcoholic liver disease.

Ethanol abuse increases gut permeability and facilitates translocation of bacterial components, such as lipopolysaccharide [38]. When Kupffer cells (KC), the resident macrophages of the liver, are exposed to these bacterial products, they become activated, produce pro-inflammatory cytokines, chemokines, and reactive oxygen species, which finally progress liver damage [38–40]. Agents that block pro-inflammatory pathways in KCs accordingly alleviated alcoholic liver diseases [38]. Depletion of KCs reduced hepatic injury in a murine model for early ethanol-induced hepatitis [41]. Steatosis, necrosis, and inflammation scores were all improved in KC depleted animal models of alcoholic liver disease [42].

KCs have a central function in lipid metabolism. Cholesterol and cholesteryl ester (CE) levels of KCs are high in comparison to parenchymal liver cells [43]. These cells react to lipids, such as ceramides, and moreover, contribute to liver steatosis [44,45].

The effect of KC depletion on the hepatic lipidome of mice with liver steatosis has not been studied in very detail so far. To the best of our knowledge, no data are available in the literature, which undertook a lipidomic profiling of Kupffer cell depleted livers, neither under normal diet nor upon a steatosis-inducing diet. Here, female mice were fed the LDC diet or a control chow for 6 weeks (Fig. 1). Phosphate buffered saline as control or clodronate liposomes were administered by intraperitoneal injection. Liver lipids were quantified by mass spectrometry. LDC feeding induced hepatic triglyceride and cholesterol amounts, and levels of these lipids were not grossly changed upon KC deficiency. Unexpectedly, KC loss increased hepatic long-chain ceramide and free cholesterol levels in LDC treated mice, suggesting a protective role of KCs in alcoholic steatosis.

## 2. Materials and methods

### 2.1. Animal experiments

Animal studies were approved by of the local animal welfare committee of Saarland University (permission number: 38/2013). Mice were housed in a 12/12 h light/dark cycle under constant conditions (temperature: 22 ± 2 °C; relative humidity: 55 ± 10%) with food and water *ad libitum*. Female mice on mixed genetic background, *i.e.* C57BL/6J and DBA/2J, were randomly divided into the experimental groups at the age of 3 weeks. The control group received normal chow (#1320, Altromin, Lage, Germany). The other group was fed the Lieber-DeCarli (#F1258SP, BioServ, Flemington, NJ, USA) diet as the only food source. The compositions of these diets are given in Table S1.

The LDC diet was prepared based on the manufacturer's instructions and Bertola et al. [46] with a magnetic stirrer and a magnetic stir bar. To one-third of the dry mix one-third of warm water was added, and mixed

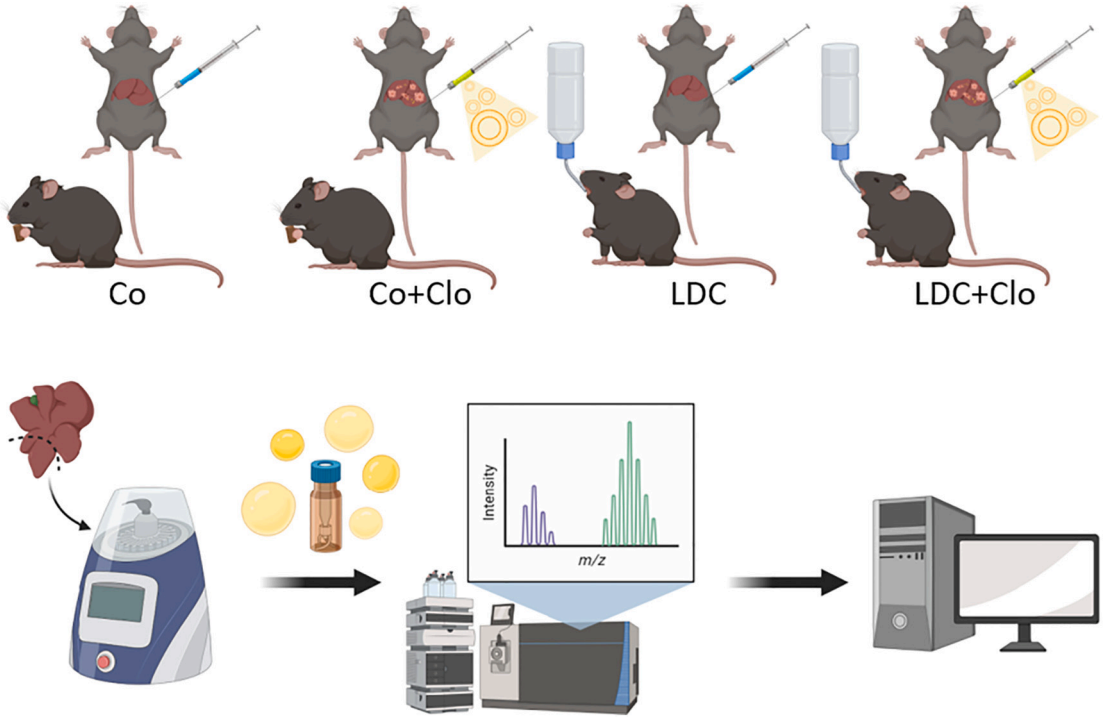


**Fig. 1.** Overview of the experimental workflow. Design of the lipidomic study displaying all experimental groups. Co: control diet, sham injections (PBS); Co+Clo: control diet, injections of clodronate (Clo) liposomes; LDC: Lieber-DeCarli diet, sham injections (PBS); LDC+Clo: Lieber-DeCarli diet, injections of clodronate liposomes; Lower panel: sample processing for lipidomics and bioinformatic analysis. Graphic was created with BioRender.com.

until the product dispersed. This step was repeated, ethanol was added, and the product was dispensed into liquid diet feeding tubes (#13260, BioServ, Flemington, NJ, USA). Mice were accustomed to the liquid diet without ethanol for 1 week. Afterwards, the ethanol concentration was raised stepwise by 1% to a final concentration of 5% according to Fengler et al. [47]. Due to unexpected spontaneous death events, the ethanol concentration was decreased to 4% during the feeding period (Table 1). In addition to the diet, animals were injected intraperitoneally with either sterile PBS (#9872, Cell Signaling, Danvers, MA, USA) or clodronate liposomes (Liposoma B.V., Amsterdam, Netherlands) according to an injection volume of 10 µl per mg body weight. Liposomes were resuspended in sterile PBS to a final concentration of 5 mg/ml clodronate in the suspension. 2 to 3 days prior to the onset of the control or LDC diet, injections were started and repeated every 5 to 7 days until mice were sacrificed at the age of 9 weeks. Total number of animals in the different diet and treatment groups are shown in Table 1.

### 2.2. Serum parameters

Whole blood was collected in 1.1 ml *Z*-Gel microtubes (#41.1500.005, Sarstedt, Nümbrecht, Germany), incubated for 1 h at room temperature and centrifuged for 10 min at 6000 ×*g* and 4 °C. The supernatant was transferred into a fresh tube and stored at −80 °C until measurement. Serum levels of alanine aminotransferase (ALT), aspartate aminotransferase (AST), cholesterol, glucose, and triglycerides (TGs) were determined by the Cobas®8000 Modular Analyzers using Roche® reagents. The serum was diluted with 0.9% NaCl prior to analysis.

**Table 1**
Feeding and treatment conditions of all experimental groups. Mice were fed either regular chow (Co) or the liquid ethanol Lieber-DeCarli diet (LDC) and underwent *i.p.* injections of sterile PBS or clodronate liposomes.

| | Co | Co + Clo | LDC | LDC + Clo |
|---|---|---|---|---|
| Injections every 5–7 days | PBS | Clo | PBS | Clo |
| + regular chow | 10 | 12 | – | – |
| + 22 days 5% + 7 days 4% EtOH | – | – | 1 | 1 |
| + 12 days 5% + 17 days 4% EtOH | – | – | 1 | – |
| + 6 days 5% + 23 days 4% EtOH | – | – | 2 | 2 |
| + 29 days 4% EtOH | – | – | 9 | 8 |
| Animals per experimental group | 10 | 12 | 13 | 11 |
| Total number of animals | 59 | | | |

PBS: Phosphate Buffered Saline; Clo: clodronate liposomes; EtOH: ethanol.

### 2.3. Measurement of endotoxins

Serum endotoxins were measured using the EndoZyme® II Recombinant Factor C (rFC) Assay (#890030, Lot# 18238, Hyglos GmbH, Bernried am Starnberger See, Germany). In contrast to the classical Limulus Amebocyte Lysate (LAL) test, a recombinant Factor C (rFC) assay has a higher specificity and sensitivity [48]. Still, sera might contain assay inhibitors, making endotoxin detection challenging, which is why heating and diluting was performed as recommended for patient sera [49]. For analysis of endotoxin levels serum of the mice was diluted 1:500 in endotoxin-free water and preheated for 15 min at 75 °C, as recommended by the manufacturer. For spike recovery, exogenous LPS (0.1 EU/ml) was added. The assay was performed according to the manufacturer's protocol. Samples with a recovery rate lower than 50% were excluded from the analysis.

### 2.4. Isolation of RNA and qPCR

Snap-frozen liver tissue was homogenized by using a high-performance dispenser (T25 digital IKA® ULTRA-TURRAX® dispersers). Subsequently, total RNA was extracted in 600 µl Qiazol® lysis reagent (#79306, Qiagen, Hilden, Germany) based on the manufacturer's instructions. DNase I digestion was performed with the Ambion DNA-free™ kit (#AM1906, Invitrogen by Thermo Fisher Scientific, Carlsbad, CA, USA) and RNA concentrations were determined using the Thermo Scientific NanoDrop Lite Spectrophotometer (Wilmington, DE, USA). 500–1000 ng of RNA was reverse transcribed into cDNA using the

high-capacity cDNA reverse transcription kit (#4368814, Applied Biosystems by Thermo Fisher Scientific, Vilnius, Lithuania) with an RNase inhibitor (RNaseOUT™, #10777019, Invitrogen by Thermo Fisher Scientific) according to the manufacturers' protocol. qPCR was performed using 5× HOT FIREPol® EvaGreen® qPCR Mix Plus (Solis BioDyne, Tartu, Estonia) according to the manufacturer's instructions to amplify the following transcripts (for: forward primer, rev: reverse primer):

*ApoA4* (for: TACGTTGCTGATGGGGTGC, rev: ATCATGCGGTCACGTAGGTC), *Clec4f* (for: CTTCGGGGAAGCAACAACTC, rev: CAAGCAACTGCACCAGAGAAC), *Elovl6* (for: ACAATGGACCTGTCAGCAAA, rev: GTACCAGTGCAGGAAGATCAGT), *Emr1* (*F4/80*, for: CTTTGGCTATGGGCTTCCAGTC, rev: GCAAGGAGGACAGAGTTTATCGTG), *Fasn* (for: GGCTGCTACAAACAGACCAT, rev: CACGGTAGAAAAGGCTCAGT), *Hmgcr* (for: ATCCAGGAGCGAACCAAGAGAG, rev: CAGAAGCCCCAAGCACAAAC), *Il1b* (for: GAGAGCCTGTGTTTTCCTCC, rev: GATGCTGCCTAATGTCCC), *Il6* (for: AAGAAATGATGGATGCTACCAAACTG, rev: GTACTCCAGAAGACCAGAGGAAATT), *Scd1* (for: GATCTCCAGTTCTTACACGACCAC, rev: CTTTCATTTCAGGACGGATGTCT), *Tnf* (for: CCATTCCTGAGTTCTGCAAAGG, rev: AGGTAGGAAGGCCTGAGATCTTATC), *Tsc22d3* (*Gilz*) (for: GGGATGTGGTTTCCGTTAAACTGGA, rev: TGCTCAATCTTGTTGTCTAGGGCCA).

Three housekeeping genes (*18S* rRNA, cyclophilin (*Ppia*), and casein kinase 2 alpha 2 (*Csnk2a2*)) were tested using the GeNorm tool and Normfinder [50,51] *Csnk2a2* was best suited as housekeeper and was amplified with the primers for: GTAAAGGACCCTGTGTCAAAG, rev: GTCAGGATCTGGTAGAGTTGCT.

All samples and standards were analyzed in triplicates and melting curve analysis was performed as a quality control.

### 2.5. Histology and staining

#### 2.5.1. Sudan III

Unfixed samples were cut on a Leica CM1950 cryostat at 8 μm, mounted onto TOMO IHC adhesive glass slides (Matsunami) and air-dried. Then, they were fixed in 4% neutral-buffered formaldehyde for 10 min and then briefly washed in aqua dest. After 1 min in 50% EtOH the slides were transferred into a Sudan III solution for 15 min.

The solution was made by adding 100 ml hot 70% EtOH to 0.25 g Sudan III (Scharlau), letting it incubate over night at 50 °C while mixing, and then, after letting it cool off, filtrating it.

The slides were briefly washed in 50% EtOH and aqua dest. Finally, it was counterstained for 5 min, each, in haematoxylin (Sanova) and tap water and then coverslipped with Aquatex (Merck).

#### 2.5.2. Oil Red O

Unfixed samples were cut on a Leica CM1950 cryostat at 8 μm, mounted onto TOMO IHC adhesive glass slides (Matsunami) and air-dried. Then, they were fixed in 4% neutral buffered formaldehyde for 10 min and then briefly washed in aqua dest, after which they were treated with 60% isopropyl alcohol for 5 min and transferred to the Oil Red O solution for 10 min.

The Oil Red O stock solution was made by dissolving 0.5 g Oil Red O (Fluka) in 100 ml 99% isopropyl alcohol. To ready it for usage it was diluted 3:2 with aqua dest and filtrated after 24 h.

The slides were washed in both 60% isopropyl alcohol and aqua dest and then counterstained in haematoxylin (Sanova) and tap water for 5 min, each. They were coverslipped with Aquatex (Merck).

### 2.6. Extraction and quantification of lipids

Samples were spiked with internal standards prior to lipid extraction (solvent of standards was removed by vacuum centrifugation). An amount of 2 mg liver (wet weight) was subjected to lipid extraction according to the protocol described by Bligh and Dyer [52] with a total chloroform volume of 2 ml. An amount of 0.5 ml of the separated chloroform phase was transferred into sample vials by a pipetting robot (Tecan Genesis RSP 150, Männedorf, Switzerland) and vacuum dried. The residues were dissolved in 1.2 ml chloroform/methanol/2-propanol (1:2:4 v/v/v) with 7.5 mM ammonium formiate. Direct flow injection analysis with a hybrid quadrupole Orbitrap mass spectrometer or a triple quadrupole mass spectrometer were used to quantify lipids, and this was described in great detail elsewhere [53–56]. Lipid species were annotated as reported [57]. Liver lipids are given as nmol/mg wet weight.

### 2.7. Statistical analysis

Data are summarized with boxplots, which display the median value, the range of the values, the lower and upper quartiles. Small circles indicate outliers greater than 1.5 times the interquartile range and stars outliers greater than 3.0 times the interquartile range. In the case that more than one lipid class was shown in a figure, the median values are displayed. Statistical analysis was done by Kruskal-Wallis-Test (SPSS Statistics 25.0 program, IBM, Leibniz Rechenzentrum, München, Germany).

### 2.8. Bioinformatic analysis

For meta-biclustering the following biclustering algorithms were used: FABIA [58], ISA [59,60], Qubic [61], Plaid [62]* and Spectral [63]* (* implemented in the biclust R package [64]). In contrast to the classical one-dimensional clustering, which can either find similar samples or similar features, biclustering simultaneously clusters samples and features, *i.e.* lipids in this case, to a subset of the full matrix. The applied meta-biclustering approach utilizes the multitude of biclustering algorithms developed and their potential to uncover different types of relations by constructing a bicluster network, in which each node is a bicluster and each edge represents a minimum similarity between the two biclusters connected. Edges are computed based on the similarity between biclusters with respect to samples and lipids. Optimal similarity cutoffs are computed from an error model, which evaluates the chance of random bicluster overlap [65]. A detailed description of the implementation can be found in Rose et al. (65). The corresponding package is available through Bioconductor as “mosbi”.

The Louvain method for community detection [66] as implemented in the igraph package [67] was used to find densely connected (*i.e.* similar with respect to sample and lipid composition) communities of biclusters, which are less connected to biclusters outside the community.

Communities with less than 4 biclusters composed of at least 5 samples were excluded to prevent a strong influence of single samples and to reduce random effects. Additionally, four bicluster communities from the full lipidome data and three from the phospho−/sphingolipid only data were not considered due to impurity with respect to sample groups.

## 3. Results

### 3.1. Hepatic expression of macrophage related genes, body weight change, serum glucose, and serum lipids of mice with alcoholic liver disease and Kupffer cell depletion

In order to assess the role of KC on alcohol-induced hepatic lipid deposition, these cells were depleted [68]. In parallel, mice were either fed a regular chow or the Lieber-DeCarli (LDC) diet for 6 weeks (Fig. 1). The mRNA levels of the KC specific gene *C-Type Lectin Domain Family 4 Member F* (*Clec4f*) [69,70] were hardly detectable in the liver of KC depleted mice confirming successful KC depletion (Fig. 2A). *F4/80* mRNA, which is highly expressed by macrophages [69], was also strongly reduced in the mice with KC loss (Fig. 2B).

Body weight change during the study period was comparable in all of the mouse groups (Fig. 2C). Serum glucose was neither altered by diet nor KC depletion (Fig. 2D). Mice fed the LDC diet had increased serum triglyceride (TG) and cholesterol levels, and this was not modified by KC

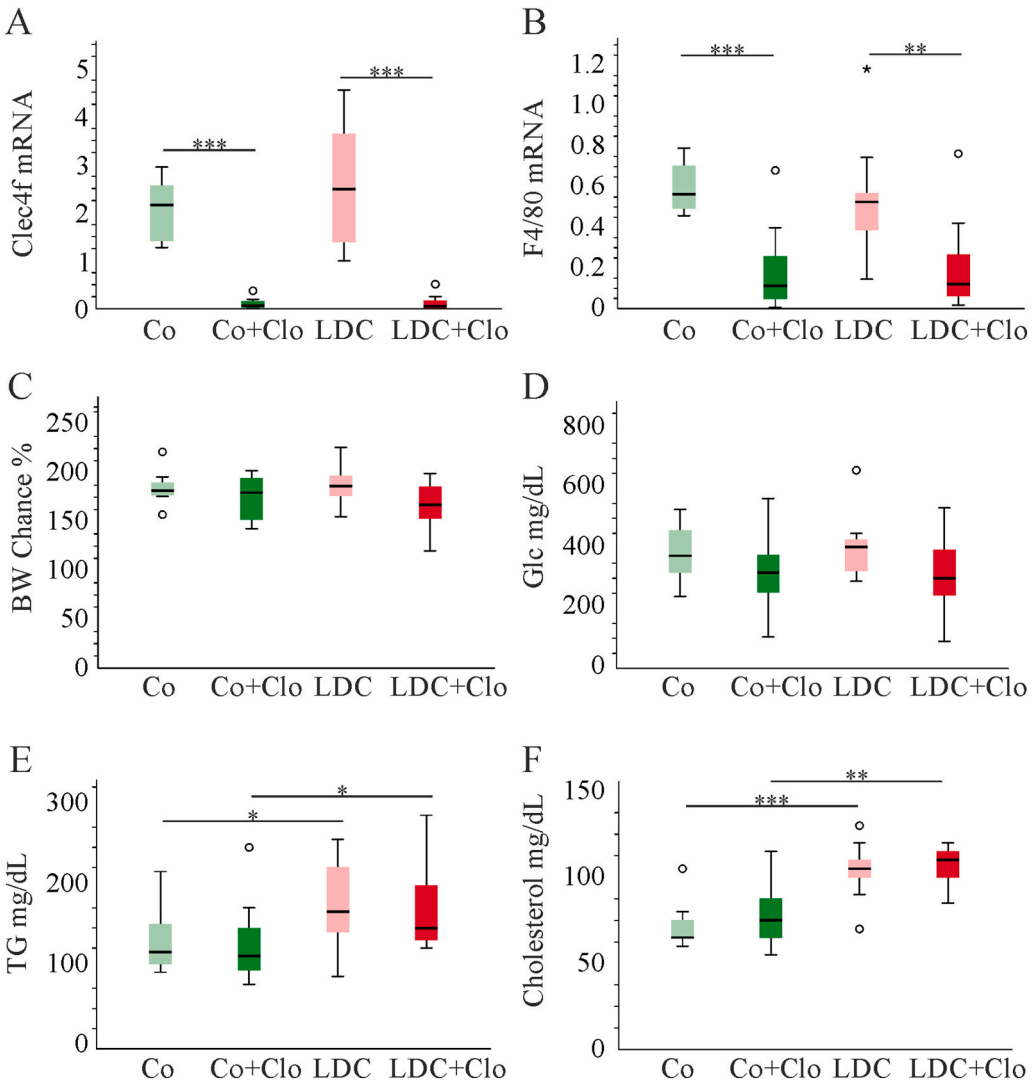


**Fig. 2.** Effect of KC depletion on macrophage genes, body weight change, and serum glucose and lipids in control mice and LDC animals. (A) Expression of *Clec4f* in the liver of control mice (Co) and animals fed alcohol (LDC), and effect of KC depletion (+Clo). (B) *F4/80* mRNA in these tissues. (C) Body weight (BW) change of the mice. (D) Serum glucose. (E) Serum triglycerides (TG) and (F) serum cholesterol. $*p < 0.05$, $**p < 0.01$, $***p < 0.001$.

ablation (Fig. 2E, F).

### 3.2. Liver weight, aminotransferase levels and hepatic inflammation of mice with alcoholic liver disease and Kupffer cell depletion

Liver weight of mice consuming ethanol was not increased (Fig. 3A). Unexpectedly, levels of alanine- and aspartate aminotransferase (ALT, AST) (Fig. 3B, C) did not rise in serum of mice fed the LDC diet. ALT and AST were higher in the KC depleted animals irrespective of the chow (Fig. 3B, C).

Expression of inflammatory cytokines is regarded as a valuable marker of liver inflammation [71]. *Tnf*, *Il6* and *Il1b* mRNA levels were, however, not induced in LDC livers (Fig. 3D - F). The decline of *Il6* and *Il1b* mRNA in KC-depleted livers is in line with the high expression of these cytokines by macrophages (Fig. 3E, F). *Il1b* mRNA was, however, not changed by KC deficiency in the LDC liver (Fig. 3F). Gene expression of the anti-inflammatory regulator glucocorticoid-induced leucine zipper (*Gilz/Tsc22d3*) was found reduced in human alcoholic hepatitis [72]. Accordingly, its expression was downregulated in the liver of mice fed the LDC diet (Fig. 3G). GILZ is abundant in KCs, and therefore declined in the control group when KCs were depleted (Fig. 3G).

Histologically scored lobular inflammation and infiltration did neither change with diet nor KC deficiency (data not shown). Hepatocyte death was higher in mice fed alcohol irrespective of KC loss (Fig. 3H).

Endotoxin concentrations were 36 (29–79) EU/ml in the sera of control mice and 46 (26–89) EU/ml in LDC animals, and therefore, were not significantly elevated in the latter group. Quantification of endotoxin is challenging and does, moreover, not provide information about its biologic activity. Thus, functional tests should be performed in the future [73].

### 3.3. Hepatic lipidome of mice fed the LDC diet and effect of Kupffer cell depletion

Dimensionality reduction using Uniform Manifold Approximation and Projection (UMAP) and hierarchical clustering using Spearman correlation as a distance measure visualized global differences between the experimental groups, clearly separating controls from LDC samples (Fig. 4). Particularly, TG, DG, and CE species were elevated in LDC-fed mice, whereas some PC and Cer species were reduced compared to Co mice. These unsupervised clustering algorithms showed that KC loss was associated with less pronounced changes in lipid composition (Fig. 4).

Meta-biclustering was used to identify possible differences in the

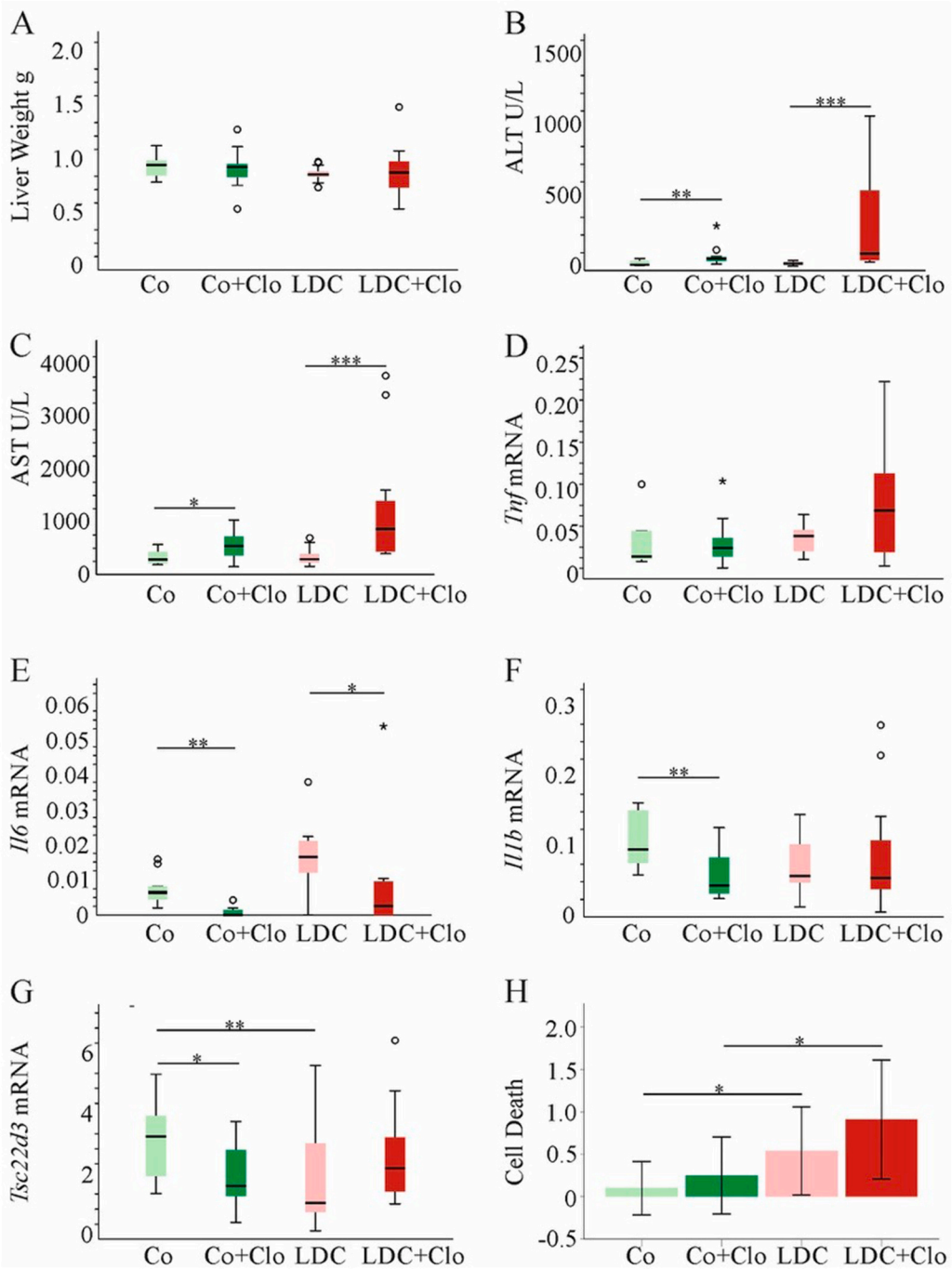


**Fig. 3.** Effect of KC depletion on liver weight, aminotransferases, hepatic inflammation and hepatocyte death in control mice and animals fed alcohol. (A) Liver weight of control mice (Co) and animals fed alcohol (LDC), and effect of KC depletion (+Clo). (B) ALT in serum of these mice. (C) AST in serum of these mice. (D) Expression of *Tnf* mRNA in the liver. (E) Expression of *Il6* mRNA in the liver. (F) Expression of *Il1b* mRNA in the liver. (G) Expression of *Tsc22d3* (*Gilz*) mRNA in the liver. (H) Cell death scores in the liver. $^{*}p < 0.05$, $^{**}p < 0.01$, $^{**}p < 0.01$, $^{***}p < 0.001$.

lipid signatures between KC-depleted and sham-treated animals within one diet. This approach was not only performed on the complete data set (Fig. 5A), but also after removing the ubiquitous intracellular storage lipids TG, DG, and CE from the analysis (reduced data set, Fig. 5B). Both strategies revealed distinct Louvain communities of biclusters discriminating all experimental groups (encircled in Fig. 5).

### 3.4. Analysis of single lipid classes and genes involved in lipid metabolism in the liver of mice with alcoholic liver disease and effect of Kupffer cell depletion

#### 3.4.1. Triglycerides, diglycerides, and cholesterol

UMAP and hierarchical clustering showed that normal and alcoholic liver greatly differed in TG and DG levels (Fig. 4) and this was significant for both lipid classes (Fig. 6A, B). According to bicluster analysis, TGs were, among all lipids, the most important ones in separating the different experimental groups (Fig. 6C, D).

H&E staining, Oil Red O, and Sudan Red staining of liver slices revealed microvesicular steatosis in animals fed the LDC diet (Fig. S1A). Steatosis score was significantly induced in the liver of animals fed with alcohol (Fig. S1B).

To describe the more subtle changes caused by KC depletion, lipid classes were analyzed separately. KC loss was associated with reduced cellular TG and DG concentrations in both groups (Fig. 6A, B). This effect was significant for DG levels in the mice fed the LDC diet (Fig. 6B).

Lipids are classified as saturated, monounsaturated (MU) and polyunsaturated (PU) fat [20,74]. Whereas MU-TGs and PU-TGs were strongly induced, the low abundant saturated TGs did not change in the

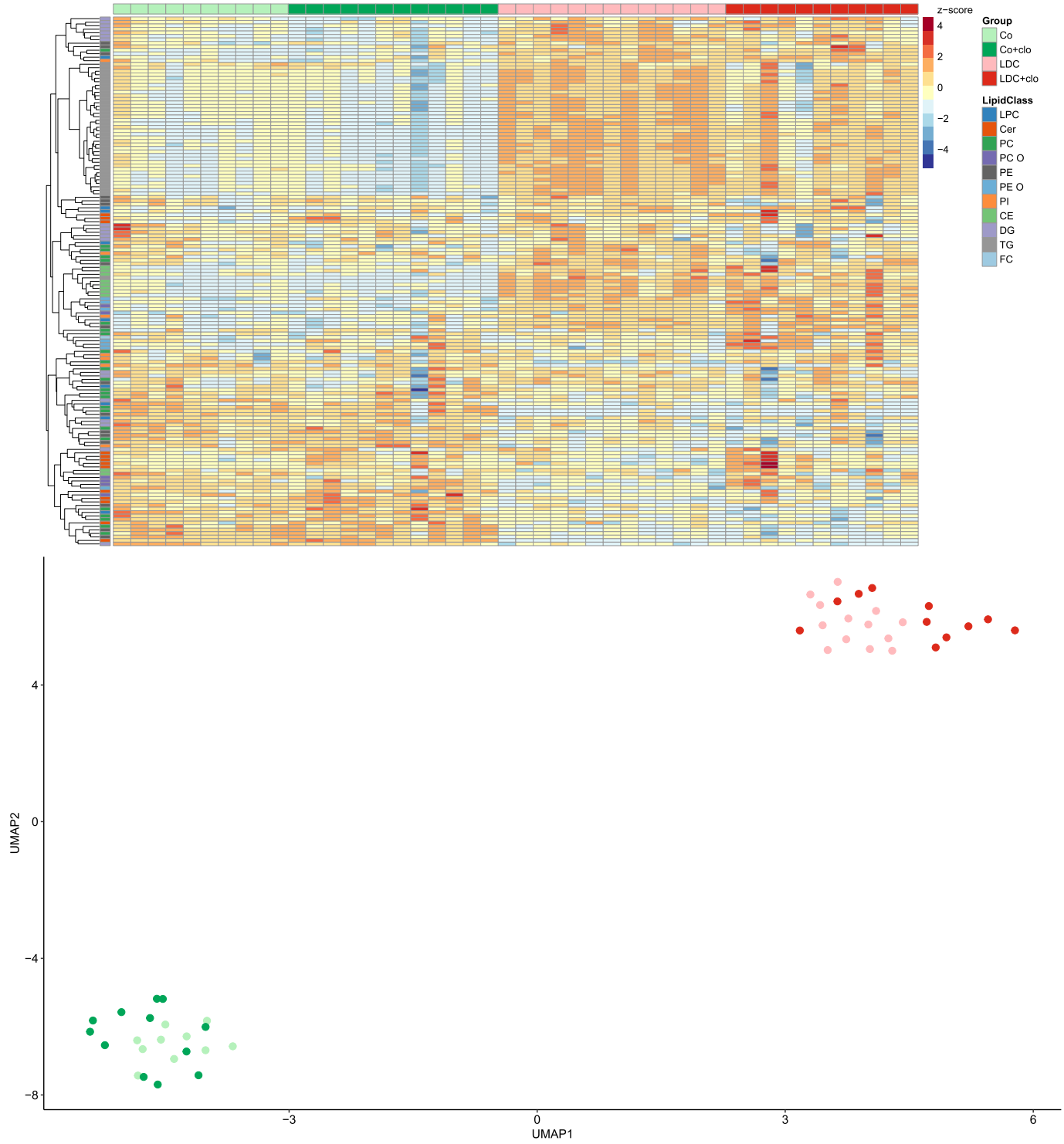


**Fig. 4.** Cluster analysis of lipid data. Hierarchical clustering (upper panel) and UMAP analysis (lower panel) of all analyzed lipid species visualizes the separation of control (blue and orange) from LDC diet (green and red) samples.

steatotic liver (Fig. 6E, F). Saturated DGs even declined in the liver of alcohol fed mice, and MU-DG and PU-DG were induced (Fig. 6G, H).

Elimination of KCs diminished levels of saturated DGs in the control group (Fig. 6G). In the LDC group this intervention had the opposite effect, and saturated DGs increased (Fig. 6G).

Loss of KCs did not change MU-DGs in both groups (Fig. 6H). KC ablation did not affect PU-DGs in the control mice but caused a reduction of PU-DGs in the alcohol group (Fig. 6H). This illustrates that the LDC livers not only accumulate TGs and DGs, but also have modified ratios of saturated to unsaturated fats.

Cholesteryl ester (CE) levels were higher in the LDC liver, and were not modified by KCs (Fig. 7A). This applied to saturated, MU-CE, and PU-CE species (Fig. 7A). Free cholesterol levels increased in the LDC liver upon KC depletion (Fig. 7B).

HMGCR is the rate-limiting enzyme in cholesterol biosynthesis [20]. *Hmgcr* mRNA levels were similar in all groups (Table 2). *Fasn* and *Scd1* mRNA expression were reduced by depletion of KCs in the control group and also declined upon alcohol feeding (Table 2). Because of a high

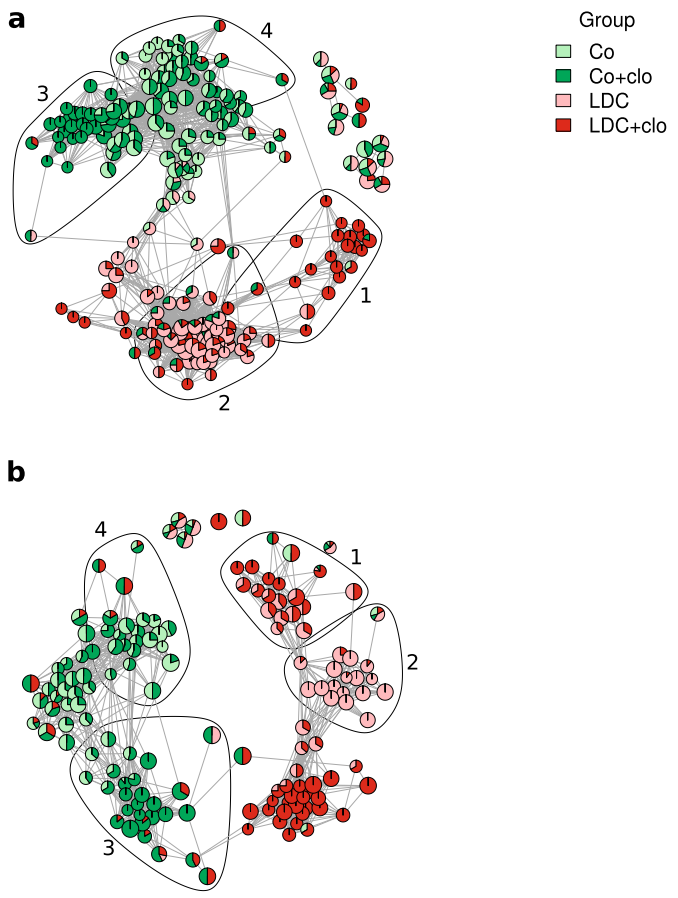


**Fig. 5.** Meta-biclustering of the complete and reduced data set. Each node represents a bicluster, the size of which is proportional to the number of samples from each experimental group. Pie chart coloring of the biclusters visualizes the proportion of the different experimental groups. Connected bicluster nodes share similar samples and lipid species. (A) Meta-bicluster analysis of the complete data set including neutral storage lipids, *i.e.* triglycerides (TG), diglycerides (DG), and cholesteryl esters (CE). (B) Meta-biclusters of the reduced data set excluding TG, DG, and CE. Both graphs revealed communities (encircled) that share similar lipid patterns. The single lipid species contained in these communities are mainly responsible for the discrimination between the diet and treatment groups.

variation in the expression levels of these genes a significant effect was only observed for the decline of *Fasn* in the controls upon KC ablation. The difference between control-fed mice and alcohol-fed animals was also significant for *Fasn* (Table 2).

A recent paper described an upregulation of *Elovl6* by alcohol consumption [75], which did not occur in the current model (Table 2). Apolipoprotein A4 is induced by ethanol in HepG2 cells and was found increased in the human alcoholic fatty liver [76,77]. Here, high apolipoprotein A4 mRNA levels were detected in ethanol-fed mice with loss of KCs (Table 2).

### 3.5. Sphingolipids in the liver of mice with alcoholic liver disease and effect of Kupffer cell depletion

There is evidence that alcohol can activate acid sphingomyelinases, which hydrolyze sphingomyelin (SM) and produces ceramide [78,79]. Sphingomyelinase activity has been reported to correlate with hepatic injury [80]. SM and ceramide level were, however, not changed in the LDC liver of the mice analyzed (Fig. 7C, D).

Ceramide levels were elevated in both groups when KCs were removed (Fig. 7D). A close association between KC depletion and the ceramide species Cer18:1;O2/22:0, 23:0, 24:0 and 24:1 was supported by the biclustering results without neutral lipids (Fig. 7G, H and Table S2). Interestingly; the long-chain ceramide Cer18:1;O2/16:0 was not included in a bicluster (Table S2).

Total ceramide levels were lower in the KC depleted LDC liver compared to the KC depleted liver of controls (Fig. 7D). Higher ceramide amounts were not accompanied by lower SM levels (Fig. 7C, D), and accordingly, the ceramide/SM ratio was increased in the liver of KC depleted mice (data not shown).

### 3.6. Phospholipids in the liver of mice with alcoholic liver disease and effect of Kupffer cell depletion

Alcohol metabolites inhibit phosphatidylethanolamine-*N*-methyltransferase and production rate of phosphatidylcholine (PC) from phosphatidylethanolamine (PE) was reduced [14,28]. However, in the current experimental model, PC and PE levels were both increased in the liver of mice fed alcohol (Fig. 8A - C). Saturated PC and PU-PC concentrations were not changed, and MU-PC was higher in the steatotic liver (Fig. 8B) Saturated PE levels were too low to obtain valid measures and unsaturated species were induced in the LDC liver (Fig. 8C and data not shown).

KC depletion did not affect hepatic PE levels (Fig. 8C). Removal of KCs caused a decline of PU-PC, and thus total PC levels, in the alcohol model (Fig. 8A, B).

The PC to PE ratio is essential for cell membrane integrity [27] and was lower in the alcohol group (Fig. 8D). Loss of KCs had no effect on this ratio in both groups (Fig. 8D).

Phosphatidylinositols, with all of the measured species having at least two double bonds, was induced in the liver of LCD fed mice and normalized upon KC depletion (Fig. 8E). Phosphatidylserine was neither changed by diet nor removal of KCs (Fig. 8F).

Our biclustering analysis independently revealed an association of PE species with the LDC diet, but no indications of KC depletion affecting PE levels were found. (Fig. 9A). PE 34:2 was in more than 50% of the biclusters (Table S2). This specific PE species seems to have diverse roles in alcoholic liver disease. Detailed evaluation of the physiological and pathophysiological function of PE 34:2 is, however, a difficult task.

Associations of the LDC diet with PI were also identified by biclustering analysis (Fig. 9B). As mentioned above, measured PIs have a high degree of desaturation, also reflected in the most frequent PI species of the afore described community.

### 3.7. PE-plasmalogens and lysophospholipids in the liver of mice with alcoholic liver disease and effect of Kupffer cell depletion

Plasmalogens may protect from oxidative stress [81] but levels of PE-plasmalogens (PE-P) were not significantly changed upon alcohol feeding or KC depletion (Fig. 10A). Interestingly, PE-P 16:0/22:6 and PE-P 18:0/22:6 were often part of biclusters (Table S2) suggesting a role of specific PE-P species in LDC steatosis.

Lysoglycerophospholipids, such as lysophosphatidylcholine (LPC) and lysophosphatidyl-ethanolamine (LPE), are generated by phospholipases from PC or PE, respectively [82]. LPC and LPE concentrations did not change in the LDC liver (Fig. 10B, C). Levels of both lipids were induced in the KC depleted liver of LCD fed mice in comparison to KC depleted controls. In the case of LPC, saturated and MU species were induced (Fig. 10D). Regarding LPE, upregulation in the LDC liver with KC ablation was caused by the increase of MU-LPE (Fig. 10E).

## 4. Discussion

The current lipidomic study revealed that TG, DG, CE, PC, PE, and PI levels were induced in the fatty liver of mice fed an LDC diet. KC depletion in these animals normalized PC and PI levels. Of note, this intervention increased FC and ceramide concentrations in alcohol fed mice. Biclustering analysis also revealed a central role of ceramide

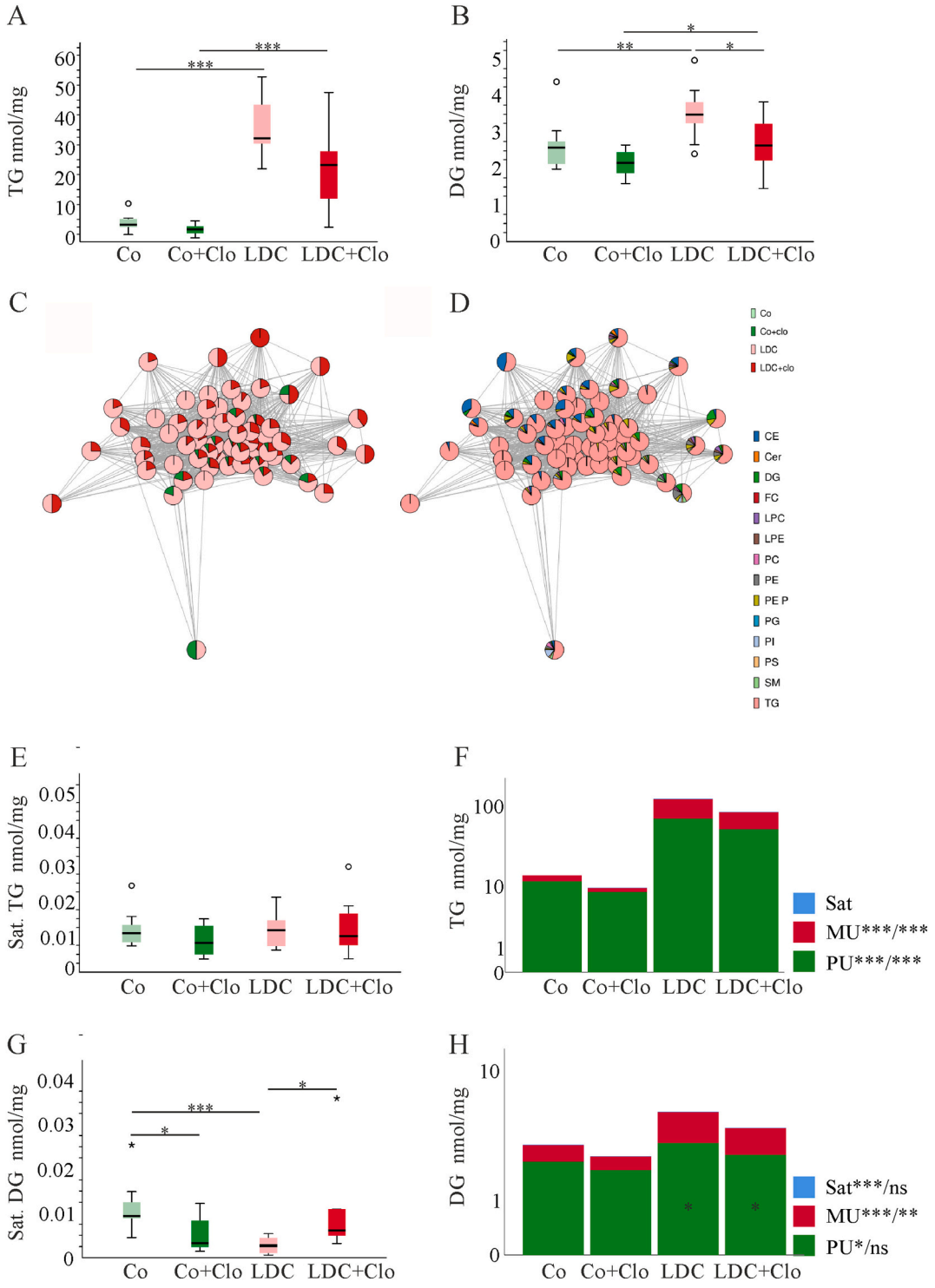


**Fig. 6.** Effect of KC depletion on triglyceride and diglyceride levels in the liver of control mice and animals fed alcohol. (A) Hepatic triglyceride (TG) levels. (B) Hepatic diglyceride (DG) levels. (C) Neutral Lipid Enriched Communities. The Community enriched in samples fed with a Lieber-DeCarli diet. Biclusters colored by the proportion of samples from each diet + treatment group. The pie-sizes in the pie-chart directly correspond to sample group distribution in the respective bicluster and its lipid profile mostly consists of TG species (D). Biclusters colored by the proportion of lipid species from each lipid class. The pie-sizes in the pie-chart directly correspond to lipid class distribution in the respective bicluster. (E) Saturated (sat) TGs. (F) Median levels of sat., monounsaturated (MU) and polyunsaturated (PU) TGs. Data are plotted on a logarithmic scale. *P*-values next to the labels refer to the differences between Co and LDC or Co+ lo and LDC+Clo, respectively. (G) Sat DGs. (H) Median levels of sat., MU- and PU-DGs. Data are plotted on a logarithmic scale. P-values next to the labels refer to the differences between Co and LDC or Co+Clo and LDC+Clo, respectively. The * in the green boxes indicates a significant effect of KC depletion on PU-DG levels in the alcohol fed mice. *$p < 0.05$, **$p < 0.01$, ***$p < 0.001$.

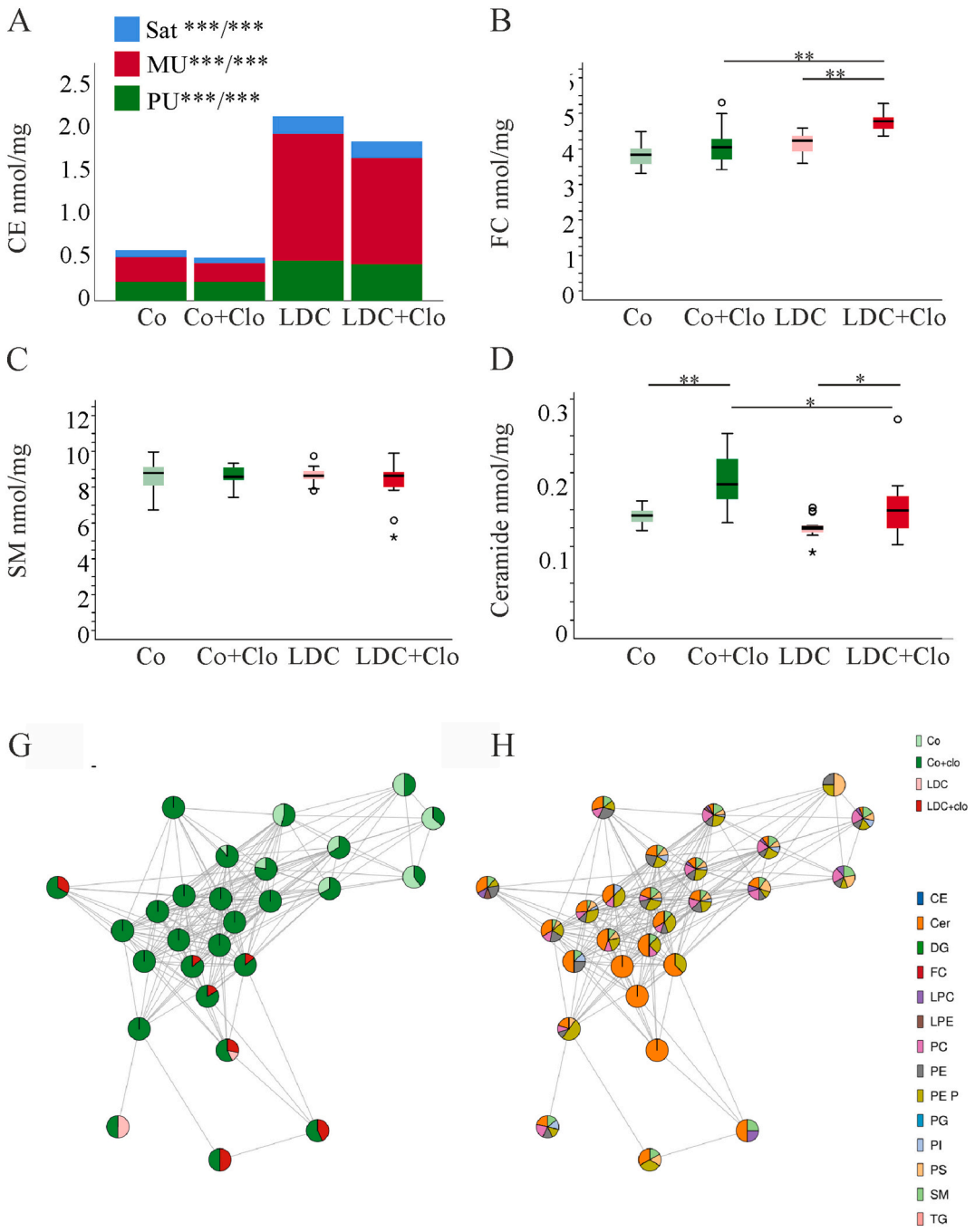


**Fig. 7.** Effect of KC depletion on cholesterol and sphingolipid levels in the liver of control mice and animals fed alcohol. (A) Median levels of saturated (sat), monounsaturated (MU) and polyunsaturated (PU) cholesteryl ester (CE). *P*-values next to the labels refer to the differences between Co and LDC or Co+Clo and LDC+Clo, respectively. (B) Free cholesterol (FC). (C) Sphingomyelin (SM). (D) Ceramide. (E) Ceramide Enriched Community. Each node represents a bicluster and each edge a minimum overlap of samples and lipid species in the two connected biclusters. Biclusters colored by the proportion of samples from each diet + treatment group. Samples are mostly KC depleted and fed the control diet. (F) Biclusters colored by the proportion of lipid species from each lipid class. The lipid signature is enriched with ceramide species. *p < 0.05, **$p$ < 0.01, ***$p$ < 0.001.

species in KC depleted LDC livers. The mice studied did not develop liver inflammation or fibrosis, and are thus a model for simple alcoholic steatosis. Present findings suggest a function of KCs in phospholipid, FC, and ceramide metabolism in alcoholic liver steatosis.

Hepatic steatosis is an early manifestation of alcohol abuse and occurs in up to 90% of the patients. Steatosis is considered a significant risk factor for progressive liver disease [83]. Hepatic lipid composition has a role in disease pathology [14], and thus, characterization of lipid classes modified by heavy drinking is essential for understanding the molecular pathways involved.

A strong accumulation of TGs and DGs was already described in the alcoholic liver [84,85], and was also observed in the current experimental model. MU-TG, PU-TG, MU-DG, and PU-DG species were induced, saturated TG species did not change and saturated DGs even declined in the liver of alcohol fed mice. In line with the current findings recent studies also reported that unsaturated DGs were higher in the alcoholic murine liver [84,85].

Expression of the lipogenic genes *Fasn* and *Scd1* even declined in the liver of the LDC diet fed animals, rather suggesting that *de novo* lipogenesis does not contribute to lipid accumulation. A role for *de novo*

**Table 2**
Expression of genes with a role in lipid metabolism. Mice were fed either regular chow (Co) or the liquid ethanol Lieber-DeCarli diet (LDC) and underwent *i.p.* injections of sterile PBS or clodronate liposomes (Clo).

| | Co | Co + Clo | LDC | LDC + Clo |
|---|---|---|---|---|
| Fatty Acid Synthase (*Fasn*) | 9.4 (2.8–17.9)[aa,b] | 0.5 (0.1–17.5)[aa] | 1.7 (0.1–84.0)[b] | 1.7 (0.2–48.5) |
| Stearoyl-CoA Desaturase 1 (*Scd1*) | 4.9 (1.5–10.4) | 1.5 (0.1–11.3) | 0.5 (0.1–37.0) | 1.4 (0.1–30.1) |
| HMG-CoA-Reductase (*Hmgcr*) | 13.9 (6.5–31.8) | 7.7 (3.5–18.1) | 10.5 (1.3–28.9) | 9.9 (2.9–37.2) |
| Fatty acid elongase (*Elovl6*) | 5.2 (3.7–8.0) | 5.7 (1.3–20.4) | 6.6 (1.8–22.6) | 7.3 (1.4–23.5) |
| Apolipoprotein A4 (*ApoA4*) | 27.2 (4.2–76.3) | 13.5 (9.7–62.2)[bb] | 22.2 (5.1–131.8)[a] | 52.3 (14.0–98.0)[a,bb] |

For variables with the same letters the difference is significant.
[a] $p < 0.05$.
[aa] $p < 0.01$.
[b] $p < 0.05$.
[bb] $p < 0.01$.

lipogenesis in alcoholic steatosis was also not evident in a further study, which suggested that uptake of fatty acids was enhanced [86]. Expression of genes for *de novo* lipogenesis is induced in the liver of ApoA4 KO rats indicating that this apolipoprotein suppresses synthesis of fatty acids [87]. *ApoA4* mRNA levels were strongly induced in the alcoholic fatty liver upon KC depletion, but this was not accompanied by lower expression of lipogenic genes.

ELOVL6, an enzyme involved in the elongating of 16 carbon fatty acids to yield 18 carbon fatty acids, was found induced in the liver of alcohol-fed rodents [75]. The mRNA levels of this enzyme were, however, similar in all of the mice analyzed herein, excluding that upregulation of this gene is a general feature of alcoholic liver disease.

Saturated fat in general harms health more than unsaturated fat [88], suggesting that the lower levels in the alcoholic liver may protect from progressive liver disease. Contrary to this assumption, convincing evidence shows that unsaturated rather than saturated fat damages the alcoholic liver. Dietary unsaturated, but not saturated, fat induced plasma ALT, liver steatosis, and inflammation [11,89,90]. In human alcoholic fatty liver an accumulation of oleate was identified [91]. PU-lipids can be easily oxidized, and thereby, bioactive lipids are produced. These molecules contribute to oxidative stress and inflammation, and progress of liver injury [90,92–94].

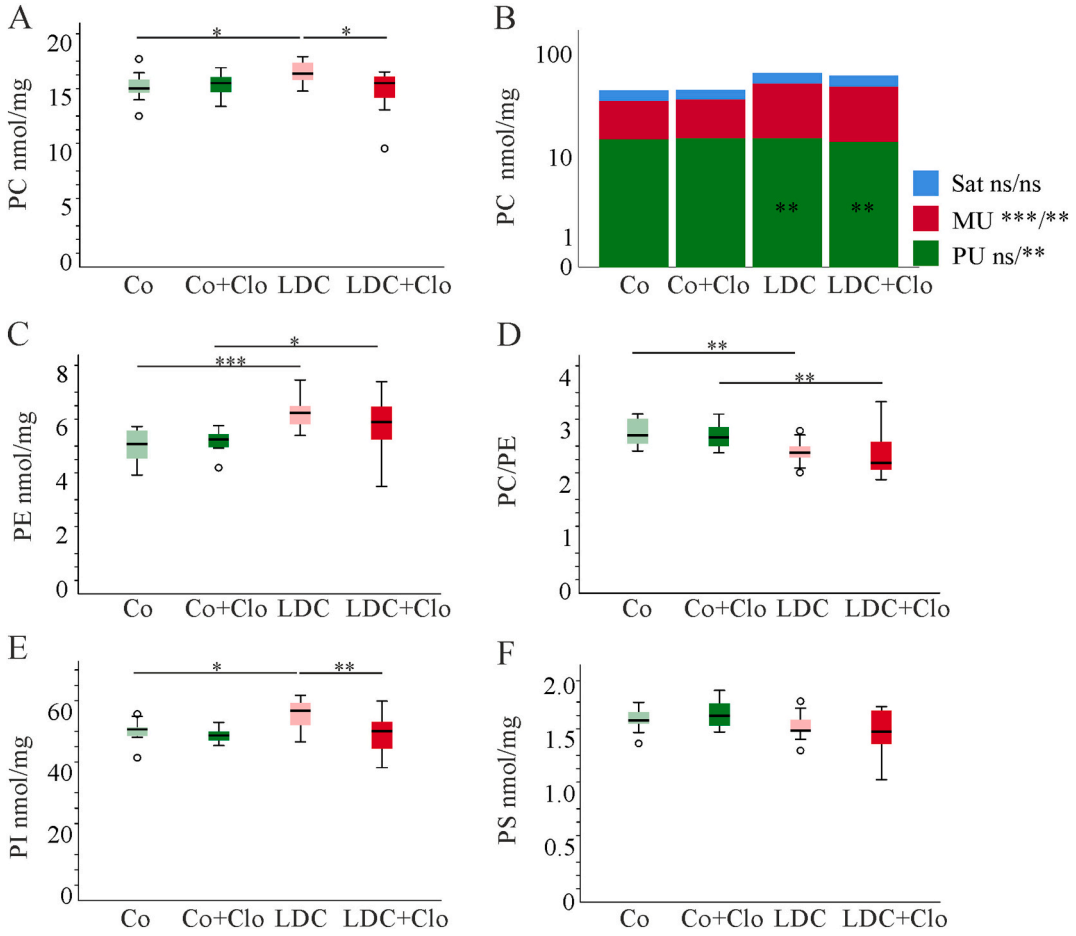


**Fig. 8.** Effect of KC depletion on phospholipid levels in the liver of control mice and animals fed alcohol. (A) Phosphatidylcholine (PC). (B) Median levels of saturated (sat), monounsaturated (MU) and polyunsaturated (PU) PC. P-values next to the labels refer to the differences between Co and LDC or Co+Clo and LDC+Clo, respectively. Not significant (ns). The ** in the green box indicates downregulation of PU-PC upon KC depletion in the alcohol fed mice. Data are plotted on a logarithmic scale. (C) Phosphatidylethanolamine (PE). (D) PC/PE ratio. (E) Phosphatidylinositol (PI). (F) Phosphatidylserine (PS). *$p < 0.05$, **$p < 0.01$, ***p $< 0.001$.

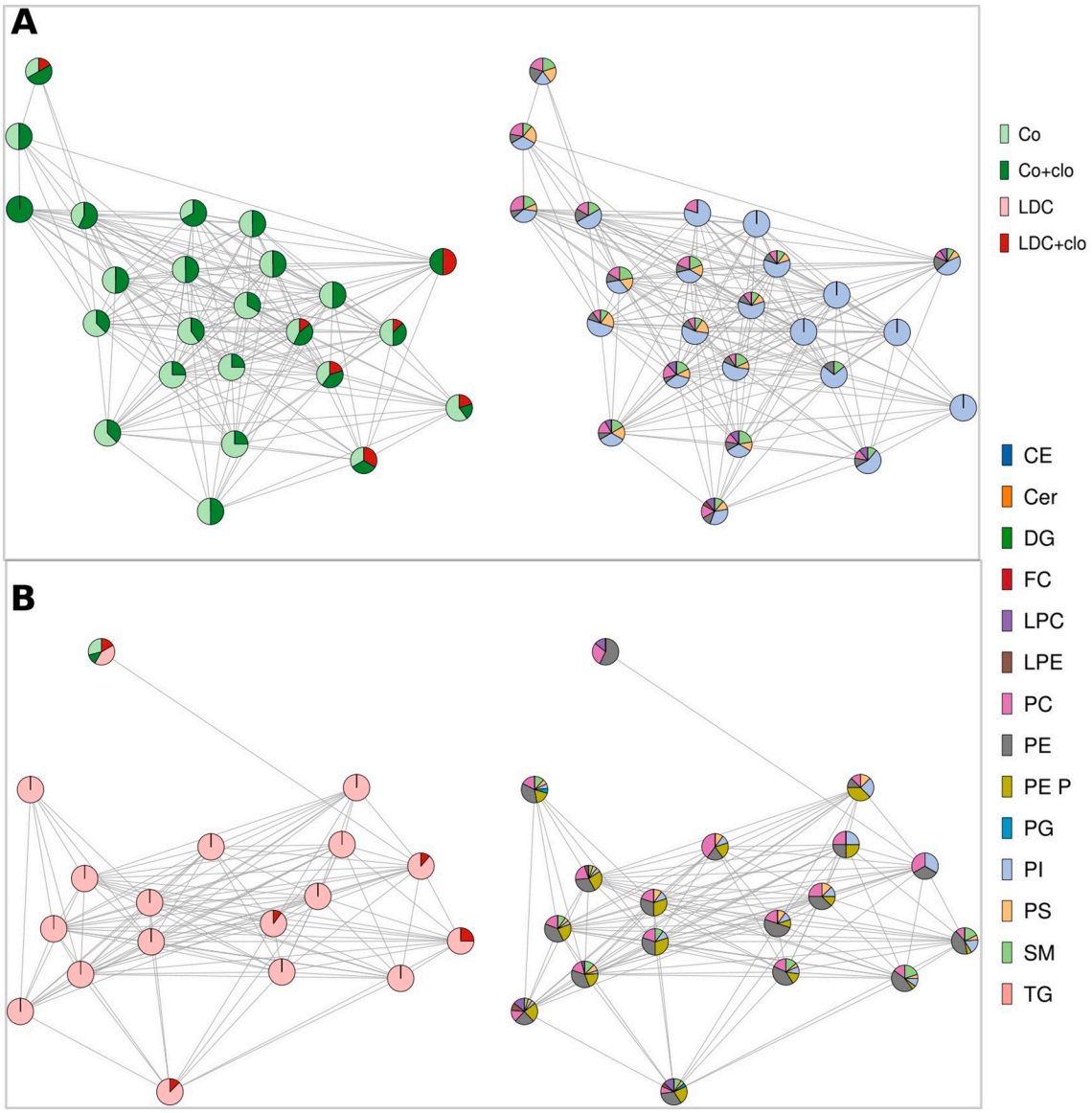


**Fig. 9.** Phospholipid Enriched Communities. Each node represents a bicluster and each edge a minimum overlap of samples and lipid species in the two connected biclusters. **A** Community enriched in samples fed with a control diet. The lipid profile of the same biclusters consists largely of PI species. **B** Biclusters of samples from the Lieber-DeCarli control group are simultaneously enriched with PE and PE-plasmalogens (PE-P) lipid species.

Accumulation of PU-lipids predisposes the liver to further injury [11,89,90]. As the mice in the current study did not display any sign of hepatic inflammation further factors may have a role herein. Adolescent (postnatal day 21) mice were fed alcohol in the current study and younger people have a lesser degree of alcohol-induced liver injury [95]. On the other hand, female mice were studied, which have a higher risk for alcoholic liver disease [96]. The final dietary alcohol concentration in the current experiments was 4% instead of the usually administered 5% [97], and this may also explain absence of liver inflammation. Hepatocyte death was nevertheless higher in the alcohol-fed mice confirming alcohol hepatotoxicity.

KC depletion was associated with a decline of TG and DG levels. This effect was not enough to normalize hepatic concentrations of these lipids in mice fed the LDC diet. Notably, a strong effect of KCs on hepatic fatty acid levels was described in animals fed a methionine-choline deficient diet to induce non-alcoholic steatohepatitis. Here, KC loss nearly abrogated fatty acid accumulation [98]. In high fat diet-fed mice hepatic triglycerides declined when KCs were depleted [44]. This anti-steatotic effect was partly explained by lower expression of *Il1b*, a cytokine shown to impair fatty acid oxidation [44].

Free fatty acids trigger the secretion of TNF by KCs, and this in turn leads to TG accumulation in hepatocytes [99]. The levels of *Tnf* mRNA did not decline upon KC depletion, although the expression of the macrophage expressed genes *Clec4f*, *Emr1 (F4/80),* and *Il6* were markedly reduced. Hepatocytes also express TNF [100] and KCs seem not to be the major producers of liver TNF. Further, in the current model, *Tnf* was not induced in the alcoholic fatty liver. This principally argues against a role for TNF in alcohol-induced liver steatosis. Notably, *Tsc22d3 (Gilz)* declined in the alcoholic liver in accordance with observations in humans [72]. Low expression of GILZ was suggested to contribute to hepatic inflammation [72]. This protein is most abundant in KCs [72] and declined in the liver of control mice when KCs had been removed. Such a downregulation was not observed in the alcoholic liver upon KC loss, and further research is needed to clarify the expression and role of GIST.

IL6 is a multifunctional cytokine and was shown to enhance lipogenesis of hepatocytes [101]. Chronically high IL6 increased the expression of lipogenic genes, such as *Fasn* and *Scd1* [102]. Hepatic *Il6*

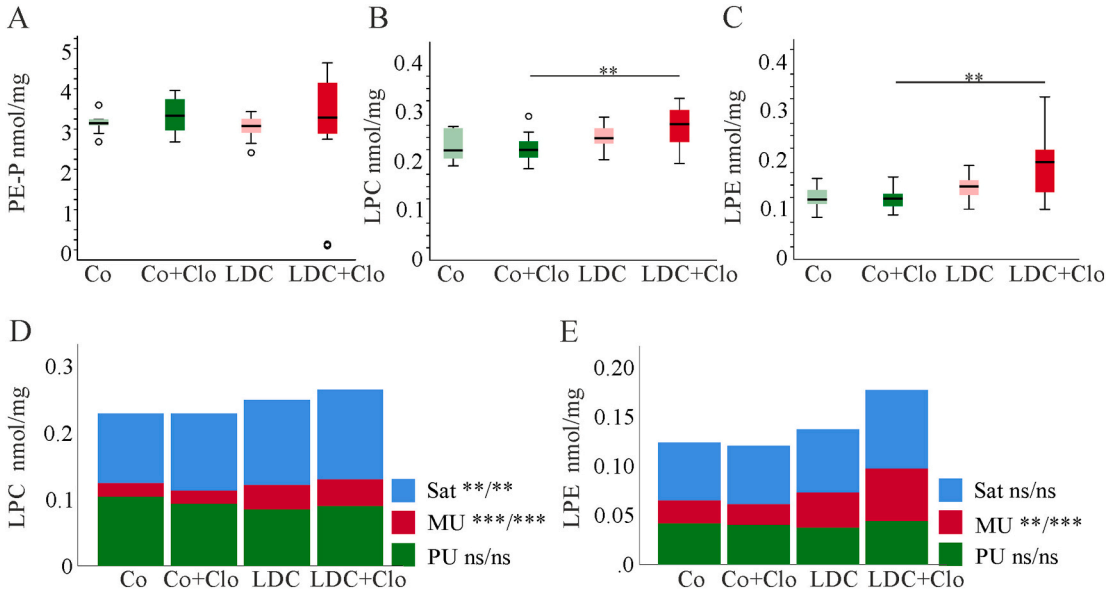


**Fig. 10.** Effect of KC depletion on PE-plasmalogen, lysoglycerophospholipid levels in the liver of control mice and animals fed alcohol. (A) PE-plasmalogen (PE-P). (B) Lysophosphatidylcholine (LPC). (C) Lysophosphatidylethanolamine (LPE). (D) Median levels of saturated (sat), monounsaturated (MU), and polyunsaturated (PU) LPC. P-values next to the labels refer to the differences between Co and LDC or Co+Clo and LDC+Clo, respectively. Not significant (ns). (E) Median levels of sat., MU- and PU-LPE. P-values next to the labels refer to the differences between Co and LDC or Co+Clo and LDC+Clo, respectively. Not significant (ns). **p < 0.01, ***p < 0.001.

mRNA declined upon KC depletion, and *Fasn* and *Scd1* expression were also decreased. Such a downregulation was not observed upon KC loss in the LDC diet fed mice. Thus, low IL6 expression in the liver may have a minor, if any, role for hepatic triglyceride levels in alcohol fed mice.

Serum IL6 is increased in obesity [103] and systemic rather than liver-expressed IL6 may be more important for hepatic lipid metabolism. Though weight gain upon alcohol feeding was reported by previous studies [86,104], this was not the case in the current study in accordance with separate investigation [85,105]. Data published so far are also discordant regarding hepatomegaly, which was observed in some but not all studies including the current one [75,86,104,105].

DGs are converted to TGs and PCs [99], and PC was also induced in the alcoholic fatty liver. A rise of PC in mice on an ethanol containing chow has been already described [85]. This previous study also identified higher PE, PI and LPE levels [85]. Concordant with that finding [85] PE and PI were also induced in the current model. Whether the rise of all of these phospholipids may protect the alcoholic liver from disease progression is unclear. PC favors the release of very low density lipoprotein particles [27], and serum TGs and cholesterol were indeed high in the alcohol-fed mice.

A decreased hepatic PC/PE ratio was associated with the development of hepatic steatosis and inflammation [106], and was described in murine and human alcoholic liver [84]. The PC/PE ratio was reduced in the present model following alcohol consumption. This suggests that the low PC/PE ratio may increase the risk for progressive liver disease upon prolonged alcohol abuse.

Fatty acids in phospholipids are mostly unsaturated, and MU-PC, MU-PE, PU-PE and PU- PI were induced in the alcoholic fatty liver. As discussed above, unsaturated fat contributes to oxidative stress in the alcoholic fatty liver [11,43,89] and higher levels of these phospholipids may be regarded as harmful.

PC regulates cellular cholesterol levels [27], and higher PC levels in the alcoholic liver may reduce the cytotoxic effects of excess cholesterol. Accumulation of cholesterol in the liver of mice fed alcohol is in line with previous findings [14]. As in the case of lipid saturation, dietary cholesterol was reported to protect from liver injury [11,14]. Further research is needed to evaluate the pathophysiological role of cholesterol deposition in the alcoholic liver.

Gene expression of the rate-limiting enzyme in cholesterol biosynthesis, HMGCR, was not induced in the alcoholic liver in accordance with a former study [104]. In the latter study the authors provide evidence for a role of impaired bile acid excretion in the hepatic accumulation of cholesterol [104].

Ceramides are a comparatively well described lipid class [107–109]. Ceramide was induced in the liver of ethanol fed mice and blockage of *de novo* ceramide synthesis improved hepatic steatosis [108]. In the present model, ceramides were not elevated in the alcoholic liver. Ceramide concentration were, however, increased upon KC cell depletion in both mouse groups. This principally indicates a protective role of KCs in the normal liver and in alcoholic liver steatosis. Very long chain ceramides cause oxidative stress and inflammation, and were induced upon depletion of KCs [20]. This observation fits the assumption that KCs are protective in alcoholic fatty liver. Increase of free cholesterol in alcoholic liver with KC loss further strengthens this hypothesis. Excess unesterified cholesterol is cytotoxic and maintenance of a steady-state is achieved by various pathways [110,111]. It is well known that macrophages participate in reverse cholesterol transport, and thereby contribute to biliary elimination of cholesterol [110]. Approaches that increased KC populations in a murine atherosclerosis model reduced cholesterol in plasma, the liver, and atherosclerotic lesion [112]. A rise of free cholesterol upon KC depletion did not occur in mice fed the control diet showing that this pathway is highly relevant when excess cholesterol is deposited in the liver.

It is noteworthy that LPC and LPE were induced in the alcohol-fed state when KCs were removed. LPC is generated by phospholipases A1 and A2 from PC, and is regarded as an inflammatory and cytotoxic lipid [113]. Phospholipase A2 also generates LPE from PE whose biological function was less well studied [82]. Saturated-LPC, MU-LPC, and MU-LPE were increased in the alcoholic liver with KC loss. On the other hand, total PE levels were not changed and only PU-PC declined upon KC ablation. This shows that production of these LPE and LPC species involves further enzymes and can not be explained by the activity of phospholipases alone. Phospholipases not only generate lysophospholipids, but also release PU fatty acids indicating that higher activity contributes to hepatic injury in the alcoholic liver [113,114].

KC ablation had little effect on the hepatic lipidome in mice fed a

control chow. As discussed above, ceramide levels were induced. Moreover, a decline of saturated DGs was observed in the control group. Saturated DGs activate protein kinase C and thereby contribute to insulin resistance [115]. Insulin signaling was, however, not affected by KC depletion in standard diet fed rats [116], and further research is needed to clarify the function of KCs in the healthy liver. Here, it has to be considered that inflammatory cytokines also contribute to hepatic insulin resistance [117]. *Il1b* was low in the liver of mice fed a control chow and devoid of KCs, and this was most likely an effect of KC loss [71]. IL1B contributes to liver steatosis, inflammation, insulin resistance, and cell death [71], suggesting that low expression is beneficial for the injured liver. Such a decline upon KC ablation was not observed in the alcoholic liver showing that *Il1b* expression of other liver resident cells was induced. Increase of ALT and AST was observed in both mouse groups with KC ablation. One study described that KCs are involved in the elimination of these enzymes and higher levels of ALT and AST are the consequence of KC depletion and not a marker of tissue injury [118]. A second analysis nevertheless found lower levels of AST and ALT in the KC depleted liver of mice fed alcohol [119]. In the present analysis serum levels of AST and ALT were not induced in alcoholic liver and increased concentrations in KC depleted animals most likely reflect impaired clearance by KCs rather than liver injury.

This work has several limitations. One is that cells were depleted by intraperitoneal injection of clodronate liposomes, and besides KCs, visceral adipose tissue macrophages are also removed by this intervention [68]. Unfortunately, visceral fat depots were not collected and expression of macrophage markers could not be examined in adipose tissues. Though it is likely that macrophages in fat were also depleted [68], for practical reasons these mice were referred to as KC-depleted animals in the manuscript. Analysis of inflammatory cytokines and enzymes with a role in lipid metabolism was only done on the mRNA level, and protein was not determined. Moreover, female mice with a mixed background were examined and conclusions may not be valid in different models. In contrast, although different backgrounds differ in their susceptibility to steatohepatitis models (47), it might rather be of advantage to use mixed genetic backgrounds to recapitulate the *per se* heterogenous human population (118). Animals had simple alcoholic steatosis, which is an early and mostly reversible state of alcoholic liver disease [2], and future studies should examine the role of KCs in advanced disease.

Despite these limitations the current study provides evidence for a central role of KCs in hepatic lipid metabolism. KC depletion in the alcoholic fatty liver led to higher levels of very long-chain ceramide and free cholesterol, which are all cytotoxic metabolites, suggesting a protective function of KCs in alcoholic liver steatosis.

## Funding sources

Contributions by N.K. and J.K.P. are funded by the Bavarian State Ministry of Science and the Arts in the framework of the Bavarian Research Institute for Digital Transformation (bidt). The results upon which this publication is based were partly funded by the Federal Ministry of Education and Research under the project number O1KU1216F (to A.K.K.) and by the Deutsche Forschungsgemeinschaft (KI 702 to A.K.K. and KE 2519 to S.M.K.).

## Data availability

The lipidomic data set is available on figshare (https://doi.org/10.6084/m9.figshare.14247971).

All code used to produce the bicluster analysis is available at: https://github.com/nklkhlr/kuppfer_cells_alcoholic_steatosis.

A general web tool is available at: https://exbio.wzw.tum.de/mosbi.

## Declaration of competing interest

The authors declare that they have no conflicts of interest with the contents of this article.

## Appendix A. Supplementary data

Supplementary data to this article can be found online at https://doi.org/10.1016/j.bbadis.2022.166398.

## References

[1] R.D. Clugston, M.A. Gao, W.S. Blaner, The hepatic lipidome: a gateway to understanding the pathogenes is of alcohol-induced fatty liver, Curr. Mol. Pharmacol. 10 (3) (2017) 195–206.
[2] E.S. Orman, G. Odena, R. Bataller, Alcoholic liver disease: pathogenesis, management, and novel targets for therapy, J. Gastroenterol. Hepatol. 28 (Suppl 1) (2013) 77–84.
[3] N. Ait-Daoud, D. Blevins, S. Khanna, S. Sharma, C.P. Holstege, P. Amin, Women and addiction: an update, Med. Clin. N.Am. 103 (4) (2019) 699–711.
[4] S. Lugonja, I. Pantic, I. Dumic, T. Milovanovic, Alcohol use by women in Serbia-a first report, Alcohol Alcohol. 56 (6) (2021) 689–694.
[5] P.K. Eagon, Alcoholic liver injury: influence of gender and hormones, World J. Gastroenterol. 16 (11) (2010) 1377–1384.
[6] S.Q. Li, P. Wang, D.M. Wang, H.J. Lu, R.F. Li, L.X. Duan, S. Zhu, S.L. Wang, Y. Y. Zhang, Y.L. Wang, Molecular mechanism for the influence of gender dimorphism on alcoholic liver injury in mice, Hum. Exp. Toxicol. 38 (1) (2019) 65–81.
[7] J.A. Clayton, F.S. Collins, Policy: NIH to balance sex in cell and animal studies, Nature 509 (7500) (2014) 282–283.
[8] N.H. Senussi, D.M. McCarthy, Simultaneous metabolic and alcohol-associated fatty liver disease (SMAFLD) and simultaneous metabolic and alcohol-associated steatohepatitis (SMASH), Ann. Hepatol. 24 (2021), 100526.
[9] F. Idalsoaga, A.V. Kulkarni, O.Y. Mousa, M. Arrese, J.P. Arab, Non-alcoholic fatty liver disease and alcohol-related liver disease: two intertwined entities, Front. Med. (Lausanne) 7 (2020) 448.
[10] J. Huang, W. Ou, M. Wang, M. Singh, Y. Liu, S. Liu, Y. Wu, Y. Zhu, R. Kumar, S. Lin, MAFLD criteria guide the subtyping of patients with fatty liver disease, Risk Manag. Healthc.Policy 14 (2021) 491–501.
[11] E. Mezey, Dietary fat and alcoholic liver disease, Hepatology 28 (4) (1998) 901–905.
[12] G. Berna, M. Romero-Gomez, The role of nutrition in non-alcoholic fatty liver disease: pathophysiology and management, Liver Int. 40 (Suppl 1) (2020) 102–108.
[13] C.P. Day, O.F. James, Hepatic steatosis: innocent bystander or guilty party? Hepatology 27 (6) (1998) 1463–1466.
[14] M. Ten Hove, L. Pater, G. Storm, S. Weiskirchen, R. Weiskirchen, T. Lammers, R. Bansal, The hepatic lipidome: from basic science to clinical translation, Adv. Drug Deliv. Rev. 159 (2020) 180–197.
[15] W. Zhong, Y. Zhao, Y. Tang, X. Wei, X. Shi, W. Sun, X. Sun, X. Yin, X. Sun, S. Kim, C.J. McClain, X. Zhang, Z. Zhou, Chronic alcohol exposure stimulates adipose tissue lipolysis in mice: role of reverse triglyceride transport in the pathogenesis of alcoholic steatosis, Am. J. Pathol. 180 (3) (2012) 998–1007.
[16] V.H. Kema, N.R. Mojerla, I. Khan, P. Mandal, Effect of alcohol on adipose tissue: a review on ethanol mediated adipose tissue injury, Adipocyte 4 (4) (2015) 225–231.
[17] R. Parker, S.J. Kim, B. Gao, Alcohol, adipose tissue and liver disease: mechanistic links and clinical considerations, Nat. Rev. Gastroenterol. Hepatol. 15 (1) (2018) 50–59.
[18] M.A. Fulham, A. Ratna, R.M. Gerstein, E.A. Kurt-Jones, P. Mandrekar, Alcohol-induced adipose tissue macrophage phenotypic switching is independent of myeloid toll-like receptor 4 expression, Am. J. Physiol. Cell Physiol. 317 (4) (2019) C687–C700.
[19] B.M. Sebastian, S. Roychowdhury, H. Tang, A.D. Hillian, A.E. Feldstein, G. L. Stahl, K. Takahashi, L.E. Nagy, Identification of a cytochrome P4502E1/Bid/C1q-dependent axis mediating inflammation in adipose tissue after chronic ethanol feeding to mice, J. Biol. Chem. 286 (41) (2011) 35989–35997.
[20] C. Buechler, C. Aslanidis, Role of lipids in pathophysiology, diagnosis and therapy of hepatocellular carcinoma, Biochim. Biophys. Acta Mol. Cell Biol. Lipids 1865 (5) (2020), 158658.
[21] L. Longato, K. Ripp, M. Setshedi, M. Dostalek, F. Akhlaghi, M. Branda, J. R. Wands, S.M. de la Monte, Insulin resistance, ceramide accumulation, and endoplasmic reticulum stress in human chronic alcohol-related liver disease, Oxidative Med. Cell. Longev. 2012 (2012), 479348.
[22] T. Ramirez, L. Longato, M. Dostalek, M. Tong, J.R. Wands, S.M. de la Monte, Insulin resistance, ceramide accumulation and endoplasmic reticulum stress in experimental chronic alcohol-induced steatohepatitis, Alcohol Alcohol. 48 (1) (2013) 39–52.
[23] J.M. Correnti, E. Juskeviciute, A. Swarup, J.B. Hoek, Pharmacological ceramide reduction alleviates alcohol-induced steatosis and hepatomegaly in adiponectin knockout mice, Am. J. Physiol. Gastrointest. Liver Physiol. 306 (11) (2014) G959–G973.

[24] H. Fernando, K.K. Bhopale, P.J. Boor, G.A. Ansari, B.S. Kaphalia, Hepatic lipid profiling of deer mice fed ethanol using (1)H and (3)(1)P NMR spectroscopy: a dose-dependent subchronic study, Toxicol. Appl. Pharmacol. 264 (3) (2012) 361–369.

[25] N. Loftus, A. Barnes, S. Ashton, F. Michopoulos, G. Theodoridis, I. Wilson, C. Ji, N. Kaplowitz, Metabonomic investigation of liver profiles of nonpolar metabolites obtained from alcohol-dosed rats and mice using high mass accuracy MSn analysis, J. Proteome Res. 10 (2) (2011) 705–713.

[26] M. Shinohara, C. Ji, N. Kaplowitz, Differences in betaine-homocysteine methyltransferase expression, endoplasmic reticulum stress response, and liver injury between alcohol-fed mice and rats, Hepatology 51 (3) (2010) 796–805.

[27] T.A. Lagace, Phosphatidylcholine: greasing the cholesterol transport machinery, Lipid Insights 8 (Suppl 1) (2015) 65–73.

[28] C.S. Lieber, S.J. Robins, J. Li, L.M. DeCarli, K.M. Mak, J.M. Fasulo, M.A. Leo, Phosphatidylcholine protects against fibrosis and cirrhosis in the baboon, Gastroenterology 106 (1) (1994) 152–159.

[29] H. Fernando, S. Kondraganti, K.K. Bhopale, D.E. Volk, M. Neerathilingam, B. S. Kaphalia, B.A. Luxon, P.J. Boor, G.A. Shakeel Ansari, (1)H and (3)(1)P NMR lipidome of ethanol-induced fatty liver, Alcohol. Clin. Exp. Res. 34 (11) (2010) 1937–1947.

[30] Z. Zhao, M. Yu, D. Crabb, Y. Xu, S. Liangpunsakul, Ethanol-induced alterations in fatty acid-related lipids in serum and tissues in mice, Alcohol. Clin. Exp. Res. 35 (2) (2011) 229–234.

[31] F. Norheim, K. Chella Krishnan, T. Bjellaas, L. Vergnes, C. Pan, B.W. Parks, Y. Meng, J. Lang, J.A. Ward, K. Reue, M. Mehrabian, T.E. Gundersen, M. Peterfy, K.T. Dalen, C.A. Drevon, S.T. Hui, A.J. Lusis, M.M. Seldin, Genetic regulation of liver lipids in a mouse model of insulin resistance and hepatic steatosis, Mol. Syst. Biol. 17 (1) (2021), e9684.

[32] L. Rein-Fischboeck, E.M. Haberl, R. Pohl, S. Feder, G. Liebisch, S. Krautbauer, C. Buechler, Variations in hepatic lipid species of age-matched male mice fed a methionine-choline-deficient diet and housed in different animal facilities, Lipids Health Dis. 18 (1) (2019) 172.

[33] Y.A. Nevzorova, Z. Boyer-Diaz, F.J. Cubero, J. Gracia-Sancho, Animal models for liver disease - a practical approach for translational research, J. Hepatol. 73 (2) (2020) 423–440.

[34] S.V. Bhave, P.L. Hoffman, N. Lassen, V. Vasiliou, L. Saba, R.A. Deitrich, B. Tabakoff, Gene array profiles of alcohol and aldehyde metabolizing enzymes in brains of C57BL/6 and DBA/2 mice, Alcohol. Clin. Exp. Res. 30 (10) (2006) 1659–1669.

[35] E.M. Boone, M.N. Cook, X. Hou, B.C. Jones, Sex and strain influence the effect of ethanol on central monoamines, J. Stud. Alcohol 58 (6) (1997) 590–599.

[36] Z. Kapasova, K.K. Szumlinski, Strain differences in alcohol-induced neurochemical plasticity: a role for accumbens glutamate in alcohol intake, Alcohol. Clin. Exp. Res. 32 (4) (2008) 617–631.

[37] https://www.jax.org/jax-mice-and-services/customer-support/technical-support/genetics-and-nomenclature/hybrid-mice.

[38] T. Zeng, C.L. Zhang, M. Xiao, R. Yang, K.Q. Xie, Critical roles of Kupffer cells in the pathogenesis of alcoholic liver disease: from basic science to clinical trials, Front. Immunol. 7 (2016) 538.

[39] A. Louvet, F. Teixeira-Clerc, M.N. Chobert, V. Deveaux, C. Pavoine, A. Zimmer, F. Pecker, A. Mallat, S. Lotersztajn, Cannabinoid CB2 receptors protect against alcoholic liver disease by regulating Kupffer cell polarization in mice, Hepatology 54 (4) (2011) 1217–1226.

[40] J. Wan, M. Benkdane, F. Teixeira-Clerc, S. Bonnafous, A. Louvet, F. Lafdil, F. Pecker, A. Tran, P. Gual, A. Mallat, S. Lotersztajn, C. Pavoine, M2 kupffer cells promote M1 Kupffer cell apoptosis: a protective mechanism against alcoholic and nonalcoholic fatty liver disease, Hepatology 59 (1) (2014) 130–142.

[41] Y.S. Roh, B. Zhang, R. Loomba, E. Seki, TLR2 and TLR9 contribute to alcohol-mediated liver injury through induction of CXCL1 and neutrophil infiltration, Am. J. Physiol. Gastrointest. Liver Physiol. 309 (1) (2015) G30–G41.

[42] D.R. Koop, B. Klopfenstein, Y. Iimuro, R.G. Thurman, Gadolinium chloride blocks alcohol-dependent liver toxicity in rats treated chronically with intragastric alcohol despite the induction of CYP2E1, Mol. Pharmacol. 51 (6) (1997) 944–950.

[43] N.R. Luzio, Lipid composition of Kupffer cells, Am. J. Physiol. Gastrointest. Liver Physiol. 196 (1959) 884–886.

[44] R. Stienstra, F. Saudale, C. Duval, S. Keshtkar, J.E. Groener, N. van Rooijen, B. Staels, S. Kersten, M. Muller, Kupffer cells promote hepatic steatosis via interleukin-1beta-dependent suppression of peroxisome proliferator-activated receptor alpha activity, Hepatology 51 (2) (2010) 511–522.

[45] T. Tang, Y. Sui, M. Lian, Z. Li, J. Hua, Pro-inflammatory activated Kupffer cells by lipids induce hepatic NKT cells deficiency through activation-induced cell death, PLoS One 8 (12) (2013), e81949.

[46] A. Bertola, O. Park, B. Gao, Chronic plus binge ethanol feeding synergistically induces neutrophil infiltration and liver injury in mice: a critical role for E-selectin, Hepatology 58 (5) (2013) 1814–1823.

[47] V.H. Fengler, T. Macheiner, S.M. Kessler, B. Czepukojc, K. Gemperlein, R. Muller, A.K. Kiemer, C. Magnes, J. Haybaeck, C. Lackner, K. Sargsyan, Susceptibility of different mouse wild type strains to develop diet-induced NAFLD/AFLD-associated liver disease, PLoS One 11 (5) (2016), e0155163.

[48] J.L. Ding, B. Ho, A new era in pyrogen testing, Trends Biotechnol. 19 (8) (2001) 277–281.

[49] Z.Y. Huang, T. Stabler, F.X. Pei, V.B. Kraus, Both systemic and local lipopolysaccharide (LPS) burden are associated with knee OA severity and inflammation, Osteoarthr. Cartil. 24 (10) (2016) 1769–1775.

[50] C.L. Andersen, J.L. Jensen, T.F. Orntoft, Normalization of real-time quantitative reverse transcription-PCR data: a model-based variance estimation approach to identify genes suited for normalization, applied to bladder and colon cancer data sets, Cancer Res. 64 (15) (2004) 5245–5250.

[51] J. Vandesompele, K. De Preter, F. Pattyn, B. Poppe, N. Van Roy, A. De Paepe, F. Speleman, Accurate normalization of real-time quantitative RT-PCR data by geometric averaging of multiple internal control genes, Genome Biol. 3 (7) (2002), RESEARCH0034.

[52] E.G. Bligh, W.J. Dyer, A rapid method of total lipid extraction and purification, Can. J. Biochem. Physiol. 37 (8) (1959) 911–917.

[53] M. Horing, C.S. Ejsing, M. Hermansson, G. Liebisch, Quantification of cholesterol and cholesteryl ester by direct flow injection high-resolution Fourier transform mass spectrometry utilizing species-specific response factors, Anal. Chem. 91 (5) (2019) 3459–3466.

[54] G. Liebisch, M. Binder, R. Schifferer, T. Langmann, B. Schulz, G. Schmitz, High throughput quantification of cholesterol and cholesteryl ester by electrospray ionization tandem mass spectrometry (ESI-MS/MS), Biochim. Biophys. Acta 1761 (1) (2006) 121–128.

[55] G. Liebisch, W. Drobnik, M. Reil, B. Trumbach, R. Arnecke, B. Olgemoller, A. Roscher, G. Schmitz, Quantitative measurement of different ceramide species from crude cellular extracts by electrospray ionization tandem mass spectrometry (ESI-MS/MS), J. Lipid Res. 40 (8) (1999) 1539–1546.

[56] G. Liebisch, B. Lieser, J. Rathenberg, W. Drobnik, G. Schmitz, High-throughput quantification of phosphatidylcholine and sphingomyelin by electrospray ionization tandem mass spectrometry coupled with isotope correction algorithm, Biochim. Biophys. Acta 1686 (1–2) (2004) 108–117.

[57] G. Liebisch, J.A. Vizcaino, H. Kofeler, M. Trotzmuller, W.J. Griffiths, G. Schmitz, F. Spener, M.J. Wakelam, Shorthand notation for lipid structures derived from mass spectrometry, J. Lipid Res. 54 (6) (2013) 1523–1530.

[58] S. Hochreiter, U. Bodenhofer, M. Heusel, A. Mayr, A. Mitterecker, A. Kasim, T. Khamiakova, S. Van Sanden, D. Lin, W. Talloen, L. Bijnens, H.W. Gohlmann, Z. Shkedy, D.A. Clevert, FABIA: factor analysis for bicluster acquisition, Bioinformatics 26 (12) (2010) 1520–1527.

[59] S. Bergmann, J. Ihmels, N. Barkai, Iterative signature algorithm for the analysis of large-scale gene expression data, Phys. Rev. E Stat. Nonlinear Soft Matter Phys. 67 (3 Pt 1) (2003), 031902.

[60] Y. Zhang, J. Xie, J. Yang, A. Fennell, C. Zhang, Q. Ma, QUBIC: a bioconductor package for qualitative biclustering analysis of gene co-expression data, Bioinformatics 33 (3) (2017) 450–452.

[61] H. Turner, T. Bailey, W. Krzanowski, Improved biclustering of microarray data demonstrated through systematic performance tests, Comput. Stat. Data Anal. 48 (2) (2005) 235–254.

[62] S. Kaiser, R. Santamaria, T. Khamiakova, M. Sill, R. Theron, L. Quintales, F. Leisch, E.De Troyer, S. Leon, biclust: BiCluster Algorithms. https://cran.r-project.org/web/packages/biclust/index.html, 2021.

[63] E.B. Fowlkes, C.L. Mallows, A method for comparing 2 hierarchical clusterings - rejoinder, J. Am. Stat. Assoc. 78 (383) (1983), 584-584.

[64] V.D. Blondel, J.L. Guillaume, R. Lambiotte, E. Lefebvre, Fast unfolding of communities in large networks, J. Stat. Mech. (2008) P10008, https://doi.org/10.1088/1742-5468/2008/10/P10008.

[65] T. Rose, T. Bechtler, O. Ciora, K. Le, F. Molnar, N. Koehler, J. Baumbach, R. Röttger, J. Pauling, MoSBi: Automated signature mining for molecular stratification and subtyping, 2021 bioRxiv Preprint.

[66] R.C. Team, R: A Language And Environment for Statistical Computing, R Foundation for Statistical Computing, Vienna, Austria, 2020. URL https://www.R-project.org/.

[67] G. Csardi, T. Nepusz, The igraph software package for complex network research, InterJ.Complex Syst. 1695 (5) (2006) 1–9.

[68] L. Bu, M. Gao, S. Qu, D. Liu, Intraperitoneal injection of clodronate liposomes eliminates visceral adipose macrophages and blocks high-fat diet-induced weight gain and development of insulin resistance, AAPS J. 15 (4) (2013) 1001–1011.

[69] C.Y. Yang, J.B. Chen, T.F. Tsai, Y.C. Tsai, C.Y. Tsai, P.H. Liang, T.L. Hsu, C.Y. Wu, M.G. Netea, C.H. Wong, S.L. Hsieh, CLEC4F is an inducible C-type lectin in F4/80-positive cells and is involved in alpha-galactosylceramide presentation in liver, PLoS One 8 (6) (2013), e65070.

[70] S.M. Kessler, J. Hoppstadter, K. Hosseini, S. Laggai, J. Haybaeck, A.K. Kiemer, Lack of Kupffer cell depletion in diethylnitrosamine-induced hepatic inflammation, J. Hepatol. 70 (4) (2019) 813–815.

[71] H. Tilg, A.R. Moschen, G. Szabo, Interleukin-1 and inflammasomes in alcoholic liver disease/acute alcoholic hepatitis and nonalcoholic fatty liver disease/nonalcoholic steatohepatitis, Hepatology 64 (3) (2016) 955–965.

[72] H. Hamdi, A. Bigorgne, S. Naveau, A. Balian, L. Bouchet-Delbos, A.M. Cassard-Doulcier, M.C. Maillot, I. Durand-Gasselin, S. Prevot, J. Delaveaucoupet, D. Emilie, G. Perlemuter, Glucocorticoid-induced leucine zipper: a key protein in the sensitization of monocytes to lipopolysaccharide in alcoholic hepatitis, Hepatology 46 (6) (2007) 1986–1992.

[73] R.S. Munford, Endotoxemia-menace, marker, or mistake? J. Leukoc. Biol. 100 (4) (2016) 687–698.

[74] E. Cabre, M.A. Gassull, Polyunsaturated fatty acid deficiency in liver diseases: pathophysiological and clinical significance, Nutrition 12 (7–8) (1996) 542–548.

[75] A. Vogle, T. Qian, S. Zhu, E. Burnett, H. Fey, Z. Zhu, A. Keshavarzian, M. Shaikh, Y. Hoshida, M. Kim, C. Aloman, Restricted immunological and cellular pathways are shared by murine models of chronic alcohol consumption, Sci. Rep. 10 (1) (2020) 2451.

[76] M. Kang, J. Kim, H.T. An, J. Ko, Human leucine zipper protein promotes hepatic steatosis via induction of apolipoprotein A-IV, FASEB J. 31 (6) (2017) 2548–2561.
[77] Y. Khodja, M.E. Samuels, Ethanol-mediated upregulation of APOA1 gene expression in HepG2 cells is independent of de novo lipid biosynthesis, Lipids Health Dis. 19 (1) (2020) 144.
[78] A. Fernandez, N. Matias, R. Fucho, V. Ribas, C. Von Montfort, N. Nuno, A. Baulies, L. Martinez, N. Tarrats, M. Mari, A. Colell, A. Morales, L. Dubuquoy, P. Mathurin, R. Bataller, J. Caballeria, M. Elena, J. Balsinde, N. Kaplowitz, C. Garcia-Ruiz, J. C. Fernandez-Checa, ASMase is required for chronic alcohol induced hepatic endoplasmic reticulum stress and mitochondrial cholesterol loading, J. Hepatol. 59 (4) (2013) 805–813.
[79] C. Muhle, C. Weinland, E. Gulbins, B. Lenz, J. Kornhuber, Peripheral acid sphingomyelinase activity is associated with biomarkers and phenotypes of alcohol use and dependence in patients and healthy controls, Int. J. Mol. Sci. 19 (12) (2018).
[80] G. Grammatikos, C. Mühle, N. Ferreiros, S. Schroeter, D. Bogdanou, S. Schwalm, G. Hintereder, J. Kornhuber, S. Zeuzem, C. Sarrazin, J. Pfeilschifter, Serum acid sphingomyelinase is upregulated in chronic hepatitis C infection and non alcoholic fatty liver disease, Biochim. Biophys. Acta 1841 (7) (2014) 1012–1020.
[81] M. Vitova, A. Palyzova, T. Rezanka, Plasmalogens - ubiquitous molecules occurring widely, from anaerobic bacteria to humans, Prog. Lipid Res. 83 (2021), 101111.
[82] S.T. Tan, T. Ramesh, X.R. Toh, L.N. Nguyen, Emerging roles of lysophospholipids in health and disease, Prog. Lipid Res. 80 (2020), 101068.
[83] T.M. Donohue Jr., Alcohol-induced steatosis in liver cells, World J. Gastroenterol. 13 (37) (2007) 4974–4978.
[84] S. Jeon, R. Carr, Alcohol effects on hepatic lipid metabolism, J. Lipid Res. 61 (4) (2020) 470–479.
[85] P. Puri, J. Xu, T. Vihervaara, R. Katainen, K. Ekroos, K. Daita, H.K. Min, A. Joyce, F. Mirshahi, H. Tsukamoto, A.J. Sanyal, Alcohol produces distinct hepatic lipidome and eicosanoid signature in lean and obese, J. Lipid Res. 57 (6) (2016) 1017–1028.
[86] R.D. Clugston, J.J. Yuen, Y. Hu, N.A. Abumrad, P.D. Berk, I.J. Goldberg, W. S. Blaner, L.S. Huang, CD36-deficient mice are resistant to alcohol- and high-carbohydrate-induced hepatic steatosis, J. Lipid Res. 55 (2) (2014) 239–246.
[87] Z. Wang, L. Wang, Z. Zhang, L. Feng, X. Song, J. Wu, Apolipoprotein A-IV involves in glucose and lipid metabolism of rat, Nutr. Metab. (Lond.) 16 (2019) 41.
[88] P.K. Luukkonen, S. Sadevirta, Y. Zhou, B. Kayser, A. Ali, L. Ahonen, S. Lallukka, V. Pelloux, M. Gaggini, C. Jian, A. Hakkarainen, N. Lundbom, H. Gylling, A. Salonen, M. Oresic, T. Hyotylainen, M. Orho-Melander, A. Rissanen, A. Gastaldelli, K. Clement, L. Hodson, H. Yki-Jarvinen, Saturated fat is more metabolically harmful for the human liver than unsaturated fat or simple sugars, Diabetes Care 41 (8) (2018) 1732–1739.
[89] A.A. Nanji, C.L. Mendenhall, S.W. French, Beef fat prevents alcoholic liver disease in the rat, Alcohol. Clin. Exp. Res. 13 (1) (1989) 15–19.
[90] D.R. Warner, H. Liu, S. Ghosh Dastidar, J.B. Warner, M.A.I. Prodhan, X. Yin, X. Zhang, A.E. Feldstein, B. Gao, R.A. Prough, C.J. McClain, I.A. Kirpich, Ethanol and unsaturated dietary fat induce unique patterns of hepatic omega-6 and omega-3 PUFA oxylipins in a mouse model of alcoholic liver disease, PLoS One 13 (9) (2018), e0204119.
[91] S.R. Cairns, T.J. Peters, Biochemical analysis of hepatic lipid in alcoholic and diabetic and control subjects, Clin. Sci. (Lond.) 65 (6) (1983) 645–652.
[92] C. Buechler, R. Pohl, C. Aslanidis, Pro-resolving molecules-new approaches to treat sepsis? Int. J. Mol. Sci. 18 (3) (2017).
[93] D.R. Warner, H. Liu, M.E. Miller, C.E. Ramsden, B. Gao, A.E. Feldstein, S. Schuster, C.J. McClain, I.A. Kirpich, Dietary linoleic acid and its oxidized metabolites exacerbate liver injury caused by ethanol via induction of hepatic proinflammatory response in mice, Am. J. Pathol. 187 (10) (2017) 2232–2245.
[94] W. Zhang, W. Zhong, Q. Sun, X. Sun, Z. Zhou, Hepatic overproduction of 13-HODE due to ALOX15 upregulation contributes to alcohol-induced liver injury in mice, Sci. Rep. 7 (1) (2017) 8976.
[95] N.A. Osna, T.M. Donohue Jr., K.K. Kharbanda, Alcoholic liver disease: pathogenesis and current management, Alcohol Res. 38 (2) (2017) 147–161.
[96] R.J. Wilkin, P.F. Lalor, R. Parker, P.N. Newsome, Murine models of acute alcoholic hepatitis and their relevance to human disease, Am. J. Pathol. 186 (4) (2016) 748–760.
[97] F. Guo, K. Zheng, R. Benede-Ubieto, F.J. Cubero, Y.A. Nevzorova, The Lieber-DeCarli diet-a flagship model for experimental alcoholic liver disease, Alcohol. Clin. Exp. Res. 42 (10) (2018) 1828–1840.
[98] S.M. Kessler, Y. Simon, K. Gemperlein, K. Gianmoena, C. Cadenas, V. Zimmer, J. Pokorny, A. Barghash, V. Helms, N. van Rooijen, R.M. Bohle, F. Lammert, J. G. Hengstler, R. Mueller, J. Haybaeck, A.K. Kiemer, Fatty acid elongation in non-alcoholic steatohepatitis and hepatocellular carcinoma, Int. J. Mol. Sci. 15 (4) (2014) 5762–5773.
[99] K.L. Diehl, J. Vorac, K. Hofmann, P. Meiser, I. Unterweger, L. Kuerschner, H. Weighardt, I. Forster, C. Thiele, Kupffer cells sense free fatty acids and regulate hepatic lipid metabolism in high-fat diet and inflammation, Cells 9 (10) (2020).
[100] B. Stojanovic, J. Milovanovic, A. Arsenijevic, B. Stojanovic, I. Strazic Geljic, N. Arsenijevic, S. Jonjic, M.L. Lukic, M. Milovanovic, Galectin-3 deficiency facilitates TNF-alpha-dependent hepatocyte death and liver inflammation in MCMV infection, Front. Microbiol. 10 (2019) 185.
[101] A. Dembek, S. Laggai, S.M. Kessler, B. Czepukojc, Y. Simon, A.K. Kiemer, J. Hoppstadter, Hepatic interleukin-6 production is maintained during endotoxin tolerance and facilitates lipid accumulation, Immunobiology 222 (6) (2017) 786–796.
[102] M. Vida, A.L. Gavito, F.J. Pavon, D. Bautista, A. Serrano, J. Suarez, S. Arrabal, J. Decara, M. Romero-Cuevas, F. Rodriguez de Fonseca, E. Baixeras, Chronic administration of recombinant IL-6 upregulates lipogenic enzyme expression and aggravates high-fat-diet-induced steatosis in IL-6-deficient mice, Dis. Model. Mech. 8 (7) (2015) 721–731.
[103] K. Eder, N. Baffy, A. Falus, A.K. Fulop, The major inflammatory mediator interleukin-6 and obesity, Inflamm. Res. 58 (11) (2009) 727–736.
[104] M.R. Lakshmanan, R.L. Veech, Short- and long-term effects of ethanol administration in vivo on rat liver HMG-CoA reductase and cholesterol 7alpha-hydroxylase activities, J. Lipid Res. 18 (3) (1977) 325–330.
[105] W.S. Blaner, M.A. Gao, H. Jiang, T.R. Dalmer, X.J. Hu, H.N. Ginsberg, R. D. Clugston, Chronic alcohol consumption decreases brown adipose tissue mass and disrupts thermoregulation: a possible role for altered retinoid signaling, Sci. Rep. 7 (2017) 43474.
[106] J. Ling, T. Chaba, L.F. Zhu, R.L. Jacobs, D.E. Vance, Hepatic ratio of phosphatidylcholine to phosphatidylethanolamine predicts survival after partial hepatectomy in mice, Hepatology 55 (4) (2012) 1094–1102.
[107] D. Hartmann, M.S. Wegner, R.A. Wanger, N. Ferreiros, Y. Schreiber, J. Lucks, S. Schiffmann, G. Geisslinger, S. Grosch, The equilibrium between long and very long chain ceramides is important for the fate of the cell and can be influenced by co-expression of CerS, Int. J. Biochem. Cell Biol. 45 (7) (2013) 1195–1203.
[108] B. Williams, J. Correnti, A. Oranu, A. Lin, V. Scott, M. Annoh, J. Beck, E. Furth, V. Mitchell, C.E. Senkal, L. Obeid, R.M. Carr, A novel role for ceramide synthase 6 in mouse and human alcoholic steatosis, FASEB J. 32 (1) (2018) 130–142.
[109] L. Yang, G.H. Jin, J.Y. Zhou, The role of ceramide in the pathogenesis of alcoholic liver disease, Alcohol Alcohol. 51 (3) (2016) 251–257.
[110] C. Buechler, S. Bauer, ATP binding cassette transporter A1 (ABCA1) associated proteins: potential drug targets in the metabolic syndrome and atherosclerotic disease? Curr. Pharm. Biotechnol. 13 (2) (2012) 319–330.
[111] I. Tabas, Consequences of cellular cholesterol accumulation: basic concepts and physiological implications, J. Clin. Invest. 110 (7) (2002) 905–911.
[112] L. Bouchareychas, J. Pirault, F. Saint-Charles, V. Deswaerte, T. Le Roy, W. Jessup, P. Giral, W. Le Goff, T. Huby, E.L. Gautier, P. Lesnik, Promoting macrophage survival delays progression of pre-existing atherosclerotic lesions through macrophage-derived apoE, Cardiovasc. Res. 108 (1) (2015) 111–123.
[113] M.S. Han, S.Y. Park, K. Shinzawa, S. Kim, K.W. Chung, J.H. Lee, C.H. Kwon, K. W. Lee, J.H. Lee, C.K. Park, W.J. Chung, J.S. Hwang, J.J. Yan, D.K. Song, Y. Tsujimoto, M.S. Lee, Lysophosphatidylcholine as a death effector in the lipoapoptosis of hepatocytes, J. Lipid Res. 49 (1) (2008) 84–97.
[114] S.H. Law, M.L. Chan, G.K. Marathe, F. Parveen, C.H. Chen, L.Y. Ke, An updated review of lysophosphatidylcholine metabolism in human diseases, Int. J. Mol. Sci. 20 (5) (2019).
[115] G.I. Shulman, Cellular mechanisms of insulin resistance, J. Clin. Invest. 106 (2) (2000) 171–176.
[116] Z. Papackova, E. Palenickova, H. Dankova, J. Zdychova, V. Skop, L. Kazdova, M. Cahova, Kupffer cells ameliorate hepatic insulin resistance induced by high-fat diet rich in monounsaturated fatty acids: the evidence for the involvement of alternatively activated macrophages, Nutr. Metab. (Lond.) 9 (2012) 22.
[117] J. Jager, M. Aparicio-Vergara, M. Aouadi, Liver innate immune cells and insulin resistance: the multiple facets of Kupffer cells, J. Intern. Med. 280 (2) (2016) 209–220.
[118] Z.A. Radi, P.H. Koza-Taylor, R.R. Bell, L.A. Obert, H.A. Runnels, J.S. Beebe, M. P. Lawton, S. Sadis, Increased serum enzyme levels associated with Kupffer cell reduction with no signs of hepatic or skeletal muscle injury, Am. J. Pathol. 179 (1) (2011) 240–247.
[119] P. Luo, F. Wang, N.K. Wong, Y. Lv, X. Li, M. Li, G.L. Tipoe, K.F. So, A. Xu, S. Chen, J. Xiao, H. Wang, Divergent roles of Kupffer cell TLR2/3 signaling in alcoholic liver disease and the protective role of EGCG, Cell. Mol. Gastroenterol. Hepatol. 9 (1) (2020) 145–160.